

1 **Examining the Effects of Anthropogenic Emissions on Isoprene-**  
2 **Derived Secondary Organic Aerosol Formation During the 2013**  
3 **Southern Oxidant and Aerosol Study (SOAS) at the Look Rock,**  
4 **Tennessee, Ground Site**

5 **S. H. Budisulistiorini<sup>1,6</sup>, X. Li<sup>1</sup>, S. T. Bairai<sup>2,†</sup>, J. Renfro<sup>3</sup>, Y. Liu<sup>4</sup>, Y. J. Liu<sup>4</sup>, K. A.**  
6 **McKinney<sup>4</sup>, S. T. Martin<sup>4</sup>, V. F. McNeill<sup>5</sup>, H. O. T. Pye<sup>6</sup>, A. Nenes<sup>7,8,9</sup>, M. E. Neff<sup>10</sup>, E. A.**  
7 **Stone<sup>10</sup>, S. Mueller<sup>2,‡</sup>, C. Knote<sup>11</sup>, S. L. Shaw<sup>12</sup>, Z. Zhang<sup>1</sup>, A. Gold<sup>1</sup>, and J. D. Surratt<sup>1</sup>**

8 [1] Department of Environmental Sciences and Engineering, Gillings School of Global Public  
9 Health, The University of North Carolina at Chapel Hill, Chapel Hill, NC, USA

10 [2] Tennessee Valley Authority, Muscle Shoals, AL, USA

11 [3] National Park Service, Gatlinburg, TN USA

12 [4] School of Engineering and Applied Sciences, Harvard University, Cambridge, MA USA

13 [5] Department of Chemical Engineering, Columbia University, NY, USA

14 [6] National Exposure Research Laboratory, US Environmental Protection Agency, Research  
15 Triangle Park, NC, USA

16 [7] School of Earth and Atmospheric Sciences, Georgia Institute of Technology, Atlanta,  
17 GA, USA

18 [8] School of Chemical and Biomolecular Engineering, Georgia Institute of Technology,  
19 Atlanta, GA, USA

20 [9] Foundation for Research and Technology, Hellas, Greece

21 [10] Department of Chemistry, University of Iowa, Iowa City, IA, USA

22 [11] Department of Experimental Meteorology, Ludwig Maximilian University of Munich,  
23 Munchen, Germany

1 [12] Electric Power Research Institute, Palo Alto, CA, USA

2 † Now at Battelle, Pueblo, CO, USA

3 ‡ Now at Ensafe, Nashville, TN, USA

4 Correspondence to: J. D. Surratt (surratt@unc.edu)

## 1 **Abstract**

2 A suite of offline and real-time gas- and particle-phase measurements was deployed at  
3 Look Rock, Tennessee (TN), during the 2013 Southern Oxidant and Aerosol Study (SOAS) to  
4 examine the effects of anthropogenic emissions on isoprene-derived secondary organic  
5 aerosol (SOA) formation. High- and low-time resolution PM<sub>2.5</sub> samples were collected for  
6 analysis of known tracer compounds in isoprene-derived SOA by gas  
7 chromatography/electron ionization-mass spectrometry (GC/EI-MS) and ultra performance  
8 liquid chromatography/diode array detection-electrospray ionization-high-resolution  
9 quadrupole time-of-flight mass spectrometry (UPLC/DAD-ESI-HR-QTOFMS). Source  
10 apportionment of the organic aerosol (OA) was determined by positive matrix factorization  
11 (PMF) analysis of mass spectrometric data acquired on an Aerodyne Aerosol Chemical  
12 Speciation Monitor (ACSM). Campaign average mass concentrations of the sum of quantified  
13 isoprene-derived SOA tracers contributed to ~9% (up to 28%) of the total OA mass, with  
14 isoprene-epoxydiol (IEPOX) chemistry accounting for ~97% of the quantified tracers. PMF  
15 analysis resolved a factor with a profile similar to the IEPOX-OA factor resolved in an  
16 Atlanta study and was therefore designated IEPOX-OA. This factor was strongly correlated  
17 ( $r^2 > 0.7$ ) with 2-methyltetrols, C<sub>5</sub>-alkene triols, IEPOX-derived organosulfates, and dimers  
18 of organosulfates, confirming the role of IEPOX chemistry as the source. On average,  
19 IEPOX-derived SOA tracer mass was ~26% (up to 49%) of the IEPOX-OA factor mass,  
20 which accounted for 32% of the total OA. A low-volatility oxygenated organic aerosol (LV-  
21 OOA) and an oxidized factor with a profile similar to 91Fac observed in areas where  
22 emissions are biogenic-dominated were also resolved by PMF analysis, whereas no primary  
23 organic aerosol (POA) sources could be resolved. These findings were consistent with low  
24 levels of primary pollutants, such as nitric oxide (NO ~0.03 ppb), carbon monoxide (CO ~116

1 ppb), and black carbon (BC  $\sim 0.2 \mu\text{g m}^{-3}$ ). Particle-phase sulfate is fairly correlated ( $r^2 \sim 0.3$ )  
2 with both methacrylic acid epoxide (MAE)/hydroxymethyl-methyl- $\alpha$ -lactone (HMML)-  
3 (henceforth called methacrolein (MACR)-derived SOA tracers) and IEPOX-derived SOA  
4 tracers, and more strongly correlated ( $r^2 \sim 0.6$ ) with the IEPOX-OA factor, in sum suggesting  
5 an important role of sulfate in isoprene SOA formation. Moderate correlation between the  
6 MACR-derived SOA tracer 2-methylglyceric acid with sum of reactive and reservoir nitrogen  
7 oxides ( $\text{NO}_y$ ;  $r^2 = 0.38$ ) and nitrate ( $r^2 = 0.45$ ) indicates the potential influence of  
8 anthropogenic emissions through long-range transport. Despite the lack of a clear association  
9 of IEPOX-OA with locally estimated aerosol acidity and liquid water content (LWC), box  
10 model calculations of IEPOX uptake using the simpleGAMMA model, accounting for the  
11 role of acidity and aerosol water, predicted the abundance of the IEPOX-derived SOA tracers  
12 2-methyltetrols and the corresponding sulfates with good accuracy ( $r^2 \sim 0.5$  and  $\sim 0.7$ ,  
13 respectively). The modeling and data combined suggest an anthropogenic influence on  
14 isoprene-derived SOA formation through acid-catalyzed heterogeneous chemistry of IEPOX  
15 in the southeastern U.S. However, it appears that this process was not limited by aerosol  
16 acidity or LWC at Look Rock during SOAS. Future studies should further explore the extent  
17 to which acidity and LWC as well as aerosol viscosity and morphology becomes a limiting  
18 factor of IEPOX-derived SOA, and their modulation by anthropogenic emissions.

## 1 **1 Introduction**

2 Atmospheric fine particulate matter ( $PM_{2.5}$ , aerosol with aerodynamic diameter  $\leq 2.5$   
3  $\mu\text{m}$ ) can scatter and/or absorb solar and terrestrial radiation as well as influence cloud  
4 formation and as a result, can markedly affect regional and global climate (IPCC, 2013). It is  
5 now also established that exposure to  $PM_{2.5}$  can have an adverse impact on human health  
6 (Dockery et al., 1993, Mauderly and Chow, 2008, Hsu et al., 2011). Organic matter (OM)  
7 comprises the largest mass fraction of  $PM_{2.5}$  and is derived largely from secondary organic  
8 aerosol (SOA) formed through atmospheric oxidation of volatile organic compounds (VOCs).  
9 SOA formation has been modeled primarily within the framework of absorptive gas-to-  
10 particle partitioning (Pankow, 1994, Odum et al., 1996), with the products of volatile and  
11 semi-volatile organic precursors decreasing in volatility during multi-generational oxidation,  
12 and condensing onto pre-existing particles or creating new particles through nucleation.  
13 Recent work has demonstrated the importance of heterogeneous (or particle-phase) chemistry  
14 in SOA formation (Jang et al., 2002, Kalberer et al., 2004, Tolocka et al., 2004, Gao et al.,  
15 2004, Surratt et al., 2006); however, chemical transport models are only just beginning to  
16 incorporate explicit details of this chemistry for specific SOA precursors (Pye et al., 2013,  
17 Karambelas et al., 2014). Although much progress has been made in recent years in  
18 identifying key biogenic and anthropogenic SOA precursors, significant gaps still remain in  
19 our knowledge of the formation mechanisms, composition and properties of SOA (Hallquist  
20 et al., 2009).

21 Isoprene (2-methyl-1,3-butadiene,  $C_5H_8$ ) is the most abundant non-methane VOC  
22 emitted into Earth's atmosphere at  $\sim 600 \text{ Tg yr}^{-1}$  (Guenther et al., 2006). The southeastern U.S.  
23 during summer is a particularly strong source of isoprene, primarily through emissions by  
24 broad-leaf trees. Although isoprene is known to influence urban ozone ( $O_3$ ) formation in the

1 southeastern U.S., only in the last decade has hydroxyl radical (OH)-initiated oxidation been  
2 recognized as leading to significant SOA formation, enhanced by the presence of  
3 anthropogenic pollutants such as nitrogen oxides ( $\text{NO}_x = \text{NO} + \text{NO}_2$ ) and sulfur dioxide ( $\text{SO}_2$ )  
4 (Claeys et al., 2004, Edney et al., 2005, Surratt et al., 2006, Kroll et al., 2006, Surratt et al.,  
5 2010). Previously, the volatility of the photochemical oxidation products had been assumed to  
6 preclude formation of  $\text{PM}_{2.5}$  from isoprene oxidation (Pandis et al., 1991, Kamens et al.,  
7 1982).

8         Recent studies have made significant strides in identifying critical intermediates in  
9 isoprene SOA formation by varying the levels of  $\text{NO}_x$  (Kroll et al., 2006, Surratt et al., 2006,  
10 Surratt et al., 2010) and acidity of sulfate aerosol (Surratt et al., 2006, Surratt et al., 2010, Lin  
11 et al., 2012, Lin et al., 2013a). The proposed role of isomeric isoprene epoxydiols (IEPOX) as  
12 key intermediates in the formation of isoprene SOA under low-nitric oxide (NO) conditions  
13 (Surratt et al., 2010, Paulot et al., 2009) has recently been confirmed in studies using authentic  
14 compounds (Lin et al., 2012, Gaston et al., 2014, Nguyen et al., 2014). Under high-NO  
15 conditions, isoprene SOA has been demonstrated to form primarily via oxidation of  
16 methacrolein (MACR) (Surratt et al., 2006) and methacryloyl peroxyxynitrate (MPAN) (Surratt  
17 et al., 2010) with methacrylic acid epoxide (MAE) (Lin et al., 2013b) and hydroxymethyl-  
18 methyl- $\alpha$ -lactone (HMML) (Nguyen et al., 2015) from the further oxidation of MACR  
19 demonstrated as reactive intermediates. Under both high- and low-NO conditions, acid-  
20 catalyzed reactive uptake and multiphase chemistry of isoprene-derived epoxides (IEPOX and  
21 MAE) as well as aqueous reactions of MACR and methyl vinyl ketone (MVK) with sulfate  
22 radical anion are now known to enhance SOA formation from isoprene (Surratt et al., 2007b,  
23 Surratt et al., 2010, Lin et al., 2013b, Schindelka et al., 2013). Recent flowtube studies on  
24 reactive uptake kinetics of *trans*- $\beta$ -IEPOX (Gaston et al., 2014), the predominant IEPOX

1 isomer formed in the photochemical oxidation of isoprene (Bates et al., 2014), have estimated  
2 an atmospheric lifetime shorter than 5 h in the presence of highly acidic aqueous aerosol (pH  
3  $\leq 1$ ). Since the predicted atmospheric lifetime of IEPOX for gas-phase oxidation is 8 – 33  
4 hours at an average OH concentration of  $10^6$  molecules  $\text{cm}^{-3}$  (Jacobs et al., 2013, Bates et al.,  
5 2014) and 11 hours for deposition (Eddingsaas et al., 2010), reactive uptake of IEPOX onto  
6 highly acidic aqueous aerosol would be a competitive or potentially dominant fate of IEPOX  
7 in the atmosphere. Recent field data from sites across the southeastern U.S. collected by (Guo  
8 et al., 2015) yielded estimates that aerosol pH ranges from 0.5–2. Consistent with  
9 expectations based on the flowtube studies (Gaston et al., 2014, Riedel et al., 2015) and pH  
10 estimates from field data, IEPOX-derived SOA has been observed to account for up to 33% of  
11 the total fine organic aerosol (OA) mass collected during summer in downtown Atlanta, GA,  
12 by analysis of data acquired on an online Aerodyne Aerosol Chemical Speciation Monitor  
13 (ACSM) (Budisulistiorini et al., 2013). Similar level of isoprene-derived SOA has been  
14 recently observed at other field sites across the southeastern U.S. using the Aerodyne high-  
15 resolution time-of-flight aerosol mass spectrometer (HR-ToF-AMS) (Xu et al., 2015). In  
16 offline chemical analysis of total fine OA mass at a rural site located in Yorkville, GA (Lin et  
17 al., 2013b), up to 20% of the OA mass could be attributed to the known IEPOX-derived SOA  
18 tracers, including the 2-methylterols (Claeys et al., 2004, Lin et al., 2012),  $\text{C}_5$ -alkene triols  
19 (Wang et al., 2005, Lin et al., 2012), *cis*- and *trans*-3-methyltetrahydrofuran-3,4-diols (Lin et  
20 al., 2012, Zhang et al., 2012b) and IEPOX-derived organosulfates (Surratt et al., 2007a,  
21 Surratt et al., 2010, Lin et al., 2012).

22 In addition to examining the effects of NO and aerosol acidity on isoprene SOA  
23 formation, the effect of varying relative humidity (RH) has recently been examined. In  
24 chamber studies on the high-NO pathway under low-RH conditions, the isoprene SOA

1 constituents 2-methylglyceric acid and corresponding oligoesters derived from MACR and its  
2 associated SOA precursors (i.e., HMML and MAE), were influenced by RH conditions  
3 (Zhang et al., 2011, Nguyen et al., 2011, Nguyen et al., 2015). However, 2-methyltetrols,  
4 which are known to be major SOA constituents formed in the low-NO pathway and minor  
5 constituents in the high-NO pathway (Edney et al., 2005, Surratt et al., 2007b), did not vary  
6 significantly with RH (Zhang et al., 2011). While RH appears to have an effect on the  
7 formation of certain isoprene SOA constituents, recent flowtube studies demonstrated that  
8 aerosol acidity has a more pronounced effect on IEPOX- and MAE-derived SOA formation  
9 than RH (Gaston et al., 2014, Riedel et al., 2015). However, field studies have yielded mixed  
10 results. At Yorkville, GA, Lin et al. (2013a) observed no strong correlation of IEPOX-derived  
11 SOA with aerosol acidity, NH<sub>3</sub> levels or liquid water content (LWC), although there was a  
12 statistically significant enhancement of IEPOX-derived SOA under high SO<sub>2</sub>-sampling  
13 scenarios. Similarly, no correlation between isoprene SOA tracers and aerosol pH or LWC  
14 was observed in the analysis of filter samples collected from field studies in Sacramento, CA,  
15 and Carson City, NV (Worton et al., 2013), and in the isoprene-derived PMF factor from field  
16 study in Centerville, AL (Xu et al., 2015). Another recent field study by Budisulistiorini et al.  
17 (2013) found weak correlation ( $r^2 = 0.22$ ) between aerosol pH and an IEPOX-OA factor  
18 resolved by positive matrix factorization (PMF) from real-time organic aerosol mass spectra  
19 data acquired on an Aerodyne ACSM.

20         Although isoprene is now recognized as a major source of SOA, the exact manner in  
21 which isoprene-derived SOA is formed in the southeastern U.S. and how it is affected by  
22 anthropogenic pollutants (i.e., NO<sub>x</sub> level, aerosol acidity, sulfate and primary aerosol  
23 loadings) remains unclear. The gap in understanding has major public health and policy  
24 implications since isoprene is emitted primarily from terrestrial vegetation and is not

1 controllable, whereas strategies to control anthropogenic pollutants can be implemented.  
2 Improving our fundamental understanding of the role of anthropogenic emissions in isoprene  
3 SOA formation will be key in improving existing air quality models, especially in the  
4 southeastern U.S. where models currently under-predict isoprene SOA formation (Foley et al.,  
5 2010, Carlton et al., 2010) and as a result will be critical to developing efficient control  
6 strategies for improving air quality. The study presented here is part of the 2013 Southeast  
7 Oxidant and Aerosol Study (SOAS) spanning 1 June – 17 July 2013 at the Look Rock (LRK),  
8 TN ground site (maps are provided in supplemental information (SI)). A major aim of SOAS  
9 was to address the issue of how exactly isoprene SOA formation occurs and the potential of  
10 anthropogenic emissions to enhance SOA formation. At the LRK ground site we approached  
11 this aim by examining the chemical composition of OA measured in real-time by the  
12 Aerodyne ACSM and subsequently applying PMF for source apportionment. We also  
13 collected PM<sub>2.5</sub> on filters and quantified tracers associated with isoprene chemistry to support  
14 the assignment of OA factors resolved from factor analyses of organic mass spectral data  
15 collected by the ACSM. We examined the potential influence of anthropogenic emissions on  
16 isoprene-derived SOA by correlation with temporal variation of anthropogenic markers  
17 monitored by collocated instruments. Finally, a photochemical box model was employed to  
18 further examine the potential interactions between SOA and anthropogenic emissions. The  
19 results of this study will help to improve model parameterizations required to bring model  
20 predictions closer to ambient observations of isoprene-derived SOA formation in the  
21 southeastern U.S.

## 1    2        **Methods**

### 2    2.1    **Site Description**

3            Fine aerosol was collected continuously from 1 June – 17 July 2013. LRK is a ridge-  
4 top site located on the northwestern edge of the Great Smoky Mountain National Park  
5 (GSMNP) downwind of Maryville and Knoxville and small farms with animal grazing areas  
6 (Figs. S1–S2). Up-slope flow carries pollutants emitted in the valley during early morning to  
7 the LRK site by mid-morning (Tanner et al., 2005). In the evening, down-slope flow  
8 accompanies a shift of wind direction to the south and east during summer that isolates the  
9 site from fresh primary emissions from the valley and allows aged-secondary species to  
10 accumulate (Tanner et al., 2005). As described in Tanner et al. (2005), particulate sulfate,  
11 black carbon (BC), organic carbon (OC), PM<sub>2.5</sub> and PM<sub>10</sub> as well as gas-phase sulfur dioxide  
12 (SO<sub>2</sub>), nitric oxide (NO), nitrogen dioxide (NO<sub>2</sub>), and sum of reactive and reservoir nitrogen  
13 oxides (NO<sub>y</sub>) were measured by a suite of collocated instruments throughout the campaign  
14 (Table S1). Meteorological measurements (RH, temperature, wind direction, and wind speed)  
15 and O<sub>3</sub> concentrations were acquired at a National Park Service (NPS) shelter across a  
16 secondary road opposite the LRK shelter.

### 17    2.2    **ACSM NR-PM<sub>1</sub> Characterization**

18            Fine ambient aerosol was sampled from the rooftop of the LRK site air-conditioned  
19 building during the SOAS campaign. The sampling inlet was approximately 6 m above the  
20 ground and equipped with a PM<sub>2.5</sub> cyclone. Sample was drawn at 3 L min<sup>-1</sup> (residence time <  
21 2 s) and dried using a Nafion drier (PD-200T-24SS, Perma Pure) to maintain RH below 10%  
22 and prevent condensation during sampling. ACSM operation parameters followed those of  
23 previous studies (Budisulistiorini et al., 2013, Budisulistiorini et al., 2014). Briefly, the

1 ACSM scanning rate was set at  $200 \text{ ms amu}^{-1}$  and data were averaged over 30 min intervals.  
2 Data were acquired using ACSM DAQ version 1438 and analyzed using ACSM Local  
3 version 1532 (Aerodyne Research, Inc.) within Igor Pro 6.3 (Wavemetrics). Calibrations for  
4 sampling flow rate, mass-to-charge ratio ( $m/z$ ), response factor of nitrate ( $\text{RF}_{\text{NO}_3}$ ), and relative  
5 ionization efficiencies of both ammonium ( $\text{RIE}_{\text{NH}_4}$ ) and sulfate ( $\text{RIE}_{\text{SO}_4}$ ) were performed three  
6 times during the campaign. Mass resolution, heater bias and ionizer voltages, and amplifier  
7 zero settings were checked and adjusted daily. A collection efficiency (CE) of 0.5 calculated  
8 using Eq. 4 of Middlebrook et al. (2012) was applied to the ACSM data in order to  
9 accommodate composition-dependent CE. Correlations of combined aerosol mass  
10 concentrations of ACSM non-refractory (NR)- $\text{PM}_{10}$  and collocated black carbon (BC) with  
11 aerosol volume concentrations of  $\text{PM}_{10}$  measured by the Scanning Electrical Mobility System-  
12 Mixing Condensation Particle Counter (SEMS-MCPC, Brechtel Manufacturing Inc.) was  
13 strong ( $r^2 = 0.89$ ) and suggested an aerosol density of  $1.52 \text{ g cm}^{-3}$  (Fig. S3), close to that  
14 reported in previous studies in Pasadena, CA (Hayes et al., 2013) and Atlanta, GA  
15 (Budisulistiorini et al., 2014). If CE of 1 is used, the estimated aerosol density is  $0.78 \text{ g cm}^{-3}$ ,  
16 which is much lower than suggested bulk organic and inorganic aerosol densities of  $1.27 \text{ g}$   
17  $\text{cm}^{-3}$  and  $1.77 \text{ g cm}^{-3}$ , respectively (Cross et al., 2007).

### 18 **2.3 OA Source Characterization**

19 OA fraction acquired by the ACSM was analysed using PMF (Paatero and Tapper,  
20 1994) written in PMF Evaluation Tool (PET v2.4) (Ulbrich et al., 2009). In this study,  
21 uncertainty of a selected solution was investigated with Seeds (varied from 0 to 100, in steps  
22 of 5), 100 bootstrapping runs, and Fpeak parameters. Details of diagnostics for each PMF  
23 analysis are given in SI (Tables S2-S3 and Figs. S4-S8). Evaluation of  $Q/Q_{\text{exp}}$  time series and  
24 mass spectra and correlation of factor solutions at Fpeak 0 with collocated measurements

1 (Figs. S4–S5, Table S3) suggests that a 3-factor solution is optimum. We selected a 3-factor  
2 solution at  $F_{\text{peak}} -0.09$  based on the quality of PMF fits and interpretability when compared  
3 to tracer time series and reference mass spectra (Table S5). The mass spectrum of a factor  
4 designated IEPOX-OA conforms closely to the IEPOX-SOA factor resolved in Atlanta, GA  
5 (Budisulistiorini et al., 2013). The mass spectrum of the second factor correlates closely with  
6 the factor identified as LV-OOA in previous studies (Ulbrich et al., 2009, Ng et al., 2011).  
7 The third factor is designated 91Fac, based on the similarity of its mass spectrum to the factor  
8 91Fac, an oxygenated factor resolved in areas dominated by biogenic emissions (Robinson et  
9 al., 2011, Chen et al., 2014).

## 10 **2.4 Gas-phase Measurements**

### 11 **2.4.1 High-Resolution Time-of-Flight Chemical Ionization Mass Spectrometry (HR- 12 ToF-CIMS) Measurements**

13 Gaseous samples were measured through an approximately 1 m length of PTFE tubing  
14 ( $\frac{1}{4}$ " outside diameter) from the sidewall of the building at flow rate of  $2 \text{ L min}^{-1}$ . The  
15 sampling line was placed to face the valley such that no structures or activity would  
16 compromise sampling. Instrument performance was maintained daily by baseline, threshold,  
17 and single ion area tuning as well as  $m/z$  calibration. The instrument was not operational  
18 during some periods of the field campaign (i.e., 13 – 16 June, 21 June – 4 July, and 14 – 16  
19 July) due to power outage, broken components, and necessary maintenances. July HR-ToF-  
20 CIMS data was corrected by comparing it to collocated MVK+MACR measured by PTR-  
21 TOF-MS (Section 2.4.2) and post-campaign calibration in order to derive a correction factor  
22 to account for decay in the micro-channel plate (MCP) detector.

1           The HR-ToF-CIMS instrument was operated in the negative ion mode using acetate  
2 ion chemistry for detection of isoprene-derived epoxides. It is henceforth referred as acetate  
3 CIMS. The acetate ion system efficiently detects small organic acids via deprotonation (Veres  
4 et al., 2008, Bertram et al., 2011), such as MAE, and some vicinal diol species, such as the  
5 IEPOX, as clusters with the reagent ion. MAE is detected as the  $[C_4H_5O_3]^-$  ion at  $m/z$  101,  
6 whereas IEPOX is detected as the  $[CH_3COO \cdot C_5H_{10}O_3]^-$  ion at  $m/z$  177 (Fig. S9). IEPOX and  
7 its gas-phase precursor, hydroxyhydroperoxides (ISOPOOH), were previously measured by  
8 CIMS with triple-quadrupole mass spectrometer that provides tandem mass spectra, as cluster  
9 ion with  $CF_3O^-$  at similar  $m/z$  and were distinguishable through their daughter ions using  
10 collision-induced dissociation (Paulot et al., 2009). Recent field and laboratory studies using  
11 acetate CIMS found that both ISOPOOH and IEPOX were observed at the same cluster ion at  
12  $m/z$  177. In our measurements, interferences of ISOPOOH to the cluster ion  $m/z$  177 could not  
13 be differentiated because we could only observe the parent ions unlike Paulot et al. (2009).  
14 Our acetate CIMS sensitivities were measured to be relatively similar towards IEPOX and  
15 ISOPOOH at  $10^{-7}$  and  $9.9 \times 10^{-8}$  signal ppt<sup>-1</sup>, respectively. However, since we operated the  
16 acetate CIMS at different voltage settings than from Farmer et al. (personal communication,  
17 2015), sensitivity of the deprotonated form of IEPOX is very low, and thus it could not be  
18 used to quantitatively measure IEPOX and/or to define the fractional contribution of IEPOX  
19 and ISOPOOH to the  $m/z$  177 signal. We synthesized ISOPOOH (see Fig. S10 for nuclear  
20 magnetic resonance (NMR) data) and measured CIMS sensitivities toward ISOPOOH and  
21 IEPOX. Results indicated that response factors of both compounds were similar (see Fig.  
22 S11). Investigation of lowering the IEPOX mixing ratio by a constant factor of total  $m/z$  177  
23 signal, which will be reported in a future study, showed that SOA tracer model correlations  
24 are not sensitive to this and only tracers mass loadings vary with the IEPOX:ISOPOOH ratio.  
25 The inability to distinguish IEPOX from ISOPOOH is a limitation in our study. Therefore, we

1 carefully note here that the  $m/z$  177 ion measured during this study represents the upper limit  
2 of the IEPOX mixing ratio due to ISOPOOH interference at an unknown fraction of the  
3 signal.

4 Gaseous IEPOX and MAE were quantified with acetate CIMS by applying laboratory-  
5 derived calibration factors. All signals were normalized to acetate ion  $[\text{CH}_3\text{COO}]^-$  at  $m/z$  59 to  
6 take into account fluctuations in signal arising from changes in pressure during the course of  
7 field sampling and calibration. Calibrations were performed before and after the SOAS  
8 campaign using synthetic *trans*- $\beta$ -IEPOX and MAE standards through dilution in a dark 10-  
9  $\text{m}^3$  indoor chamber at the University of North Carolina (UNC) (Lin et al., 2012). Synthetic  
10 procedures for *trans*- $\beta$ -IEPOX and MAE have been described previously (Zhang et al., 2012b,  
11 Lin et al., 2013b). A known concentration of epoxide standard was injected into a 10-mL  
12 glass manifold using glass microliter syringes. The manifold was wrapped with heating tape  
13 and flushed with heated  $\text{N}_2$  (g) at  $5 \text{ L min}^{-1}$  for at least 2 hours to the indoor chamber being  
14 sampled by the HR-ToF-CIMS until ion signals associated with MAE and IEPOX stabilized.  
15 We assumed unit injection efficiency of the epoxides through the glass chamber and into the  
16 chamber in calculating the chamber epoxide mixing ratios. Subsequently, we performed  
17 standard dilution of the acetate CIMS sample flow by using a T-piece in an  $\text{N}_2$  (g) flow  
18 controlled by eight different micro-orifices to obtain an eight-point calibration curve. During  
19 the course of the calibration experiments, we accounted for the fact that we would lose 14 and  
20 3% of IEPOX and MAE, respectively. Wall loss rates for IEPOX and MAE have been  
21 measured in the chamber and are  $5.91 \times 10^{-5} \text{ s}^{-1}$  and  $1.12 \times 10^{-5} \text{ s}^{-1}$ , respectively (Riedel et al.,  
22 2015). The chamber was sampled continuously at  $2 \text{ L min}^{-1}$  for measurement of gaseous  
23 products by acetate CIMS and at  $0.36 \text{ L min}^{-1}$  for aerosol measurements by SEMS-MCPC to  
24 ensure that the chamber was particle free. Additionally, no particle nucleation events or

1 significant particle loadings were observed over the course of calibrations. Normalized  $m/z$   
2 177 and 101 ions were plotted against epoxide mixing ratios of eight-point standards;  
3 however, only four-point standards were used for IEPOX calibration due to non-linearity.  
4 Slopes of the fittings were used as calibration factors for the field measurements (Fig. S12).  
5 Field calibrations were not performed due to the unavailability of IEPOX and MAE  
6 permeation tube systems.

#### 7 **2.4.2 Proton Transfer Reaction Time-of-Flight Mass Spectrometry (PTR-TOF-MS)**

8 A proton-transfer-reaction time-of-flight mass spectrometer (PTR-TOF-MS 8000,  
9 Ionicon Analytik GmbH, Austria) equipped with switchable reagent ion capacity was used to  
10 measure the concentrations of gaseous organic species at the site. Ambient air was sampled  
11 from an inlet mounted on a tower ca. 2 m above the rooftop of the LRK site building through  
12 a 6.35 mm OD PFA sampling line at 4-5 standard L min<sup>-1</sup>. A 2.0- $\mu$ m pore size 47-mm  
13 diameter Zefluor teflon filter (Pall Corporation) at the inlet removed particles from the sample  
14 flow. The PTR-TOF-MS sub-sampled from this flow at a rate of 0.25 sLpm, resulting in a  
15 total inlet transit time of ca. 1-2 s.

16 PTR-TOF-MS has been described previously by Jordan et al. (2009a, 2009b) and  
17 Graus et al. (2010) and was operated in this study as described in Liu et al. (2013). H<sub>3</sub>O<sup>+</sup>  
18 reagent ions were used to selectively ionize organic molecules in the sample air. A high-  
19 resolution TOF detector (Tofwerk AG, Switzerland) was used to analyze the reagent and  
20 product ions and allowed for exact identification of the ion molecular formula (mass  
21 resolution >4000). The instrument was operated with a drift tube temperature of 80°C and a  
22 drift tube pressure of 2.35 mbar. In H<sub>3</sub>O<sup>+</sup> mode, the drift tube voltage was set to 520 V,  
23 resulting in an E/N of 120 Td (E, electric field strength; N, number density of air in the drift  
24 tube; unit, Townsend, Td; 1 Td = 10<sup>-17</sup> V cm<sup>2</sup>). PTR-TOF-MS spectra were collected at a

1 time resolution of 10s. Mass calibration was performed every 2 min with data acquisition  
2 using the Tof-Daq v1.91 software (Tofwerk AG, Switzerland).

3 A calibration system was used to establish the instrument sensitivities to VOCs. Gas  
4 standards (Scott Specialty Gases) were added into a humidified zero air flow at controlled  
5 flow rates. Every 3 h the inlet flow was switched to pass through a catalytic converter  
6 (platinum on glass wool heated to 350°C) to remove VOCs and establish background  
7 intensities.

## 8 **2.5 Filter Sampling Methods and Offline Chemical Analyses**

9 PM<sub>2.5</sub> samples were collected on pre-baked Tissuquartz™ Filters (Pall Life Sciences,  
10 8 × 10 in) with three high-volume PM<sub>2.5</sub> samplers (Tisch Environmental, Inc.). All high-  
11 volume PM<sub>2.5</sub> samplers were equipped with cyclones operated at 1 m<sup>3</sup> min<sup>-1</sup>. One high-volume  
12 sampler collected PM<sub>2.5</sub> for 23 hours (08:00 to 07:00 the next day, local time), while the two  
13 remaining samplers collected PM<sub>2.5</sub> in two cycles. When the sampling schedules were daytime  
14 (08:00 – 19:00, local time) and nighttime (20:00 – 07:00, local time), the collection cycle and  
15 samples are defined as regular day-night sampling periods and samples. On selected days (10  
16 – 12 June, 14 – 16 June, 29 – 30 June, and 9 – 16 July), when high levels of isoprene, sulfate  
17 (SO<sub>4</sub><sup>2-</sup>), and NO<sub>x</sub> were predicted at the LRK site by FLEXPART and MOZART model  
18 simulations (see SI), PM<sub>2.5</sub> were collected more frequently (08:00 – 11:00, 12:00 – 15:00,  
19 16:00 – 19:00, and 20:00 – 07:00, local time) to capture the effects of anthropogenic pollution  
20 on isoprene SOA formation at higher time resolution by offline techniques. Such days are  
21 defined as intensive sampling periods and the samples as intensive samples. Forty-seven 23-  
22 hour integrated and two sets of 64 intensive and 59 day-night filter samples were collected  
23 over the six-week period of the campaign and stored at -20°C until analysis. Field blanks were

1 collected weekly by placing pre-baked quartz filters into the high-volume PM<sub>2.5</sub> samplers for  
2 15 min and then removing and storing them under the same conditions as the field samples.

### 3 **2.5.1 Instrumentation**

4 Gas chromatography/electron ionization-mass spectrometry (GC/EI-MS) was  
5 performed on a Hewlett-Packard (HP) 5890 Series II Gas Chromatograph equipped with an  
6 Econo-Cap<sup>®</sup>-EC<sup>®</sup>-5 Capillary Column (30 m × 0.25 mm ID; 0.25 μm film thickness) coupled  
7 to an HP 5971A Mass Selective Detector. GC/EI-MS operating conditions and temperature  
8 program are provided in Surratt et al. (2010).

9 Ultra performance liquid chromatography/diode array detector-electrospray ionization  
10 high-resolution quadrupole time-of-flight mass spectrometry (UPLC/DAD-ESI-HR-  
11 QTOFMS) was performed on an Agilent 6500 series system equipped with a Waters Acquity  
12 UPLC HSS T3 column (2.1 × 100 mm, 1.8 μm particle size). UPLC/DAD-ESI-HR-QTOFMS  
13 operating conditions are described in Zhang et al. (2011).

### 14 **2.5.2 Isoprene-derived SOA Tracer Quantification**

15 Detailed filter extraction procedures are provided in Lin et al. (2013a). Briefly, from  
16 each filter two 37-mm punches (one for analysis by GC/EI-MS and one for UPLC/DAD-ESI-  
17 HR-QTOFMS analysis) were extracted in separate pre-cleaned scintillation vials with 20 mL  
18 high-purity methanol (LC-MS Chromasolv-grade<sup>®</sup>, Sigma Aldrich) by sonication for 45 min.  
19 Filter extracts were then filtered through 0.2-μm syringe filters (Acrodisc<sup>®</sup> PTFE membrane,  
20 Pall Life Sciences) to remove suspended filter fibers and insoluble particles, and then gently  
21 blown down to dryness under an N<sub>2</sub> (g) stream at room temperature.

22 The known IEPOX-derived SOA tracers, 2-methyltetrols (Claeys et al., 2004), C<sub>5</sub>-  
23 alkene triols (Wang et al., 2005), *cis*- and *trans*-3-methyltetrahydrofuran-3,4-diols (3-

1 MeTHF-3,4-diols) (Lin et al., 2013b), and IEPOX-derived dimers (Surratt et al., 2006), and  
2 the known MAE-derived SOA tracer, 2-methylglyceric acid (2-MG) (Edney et al., 2005),  
3 were identified by GC/EI-MS immediately following trimethylsilylation. Derivatization was  
4 performed by reaction with 100  $\mu$ L of BSTFA + TMCS (99:1, v/v, Supelco) and 50  $\mu$ L of  
5 pyridine (anhydrous, 99.8%, Sigma Aldrich) at 70°C for 1 hour. 1  $\mu$ L of derivatized sample  
6 was directly analyzed. Base peak ions of the corresponding tracers,  $m/z$  219 for 2-  
7 methyltetrols,  $m/z$  231 for C<sub>5</sub>-alkene triols,  $m/z$  262 for 3-MeTHF-3,4-diols,  $m/z$  335 for  
8 dimers, and  $m/z$  219 for 2-MG, were quantified using authentic standards of 2-methyltetrols  
9 (50:50, v/v, 2-C-methylerythritol and 2-C-methylthreitol), *cis*- and *trans*-3-MeTHF-3,4-diols,  
10 and 2-MG. The C<sub>5</sub>-alkene triols and dimers were quantified by the response factor obtained  
11 for the synthetic 2-methyltetrols. Synthetic procedures for *cis*- and *trans*-3-MeTHF-3,4-diols  
12 have been described previously by Zhang et al. (2012b). Synthesis of the tetrol mixture will  
13 be described in a forthcoming publication; the <sup>1</sup>H NMR trace (Figure S13) shows a 1.2:1 2-C-  
14 methylerythritol and 2-C-methylthreitol of >99% purity.

15 Organosulfates, including the 2-methyltetrol sulfate esters ( $[\text{C}_3\text{H}_{11}\text{O}_7\text{S}]^-$ ,  $m/z$  215),  
16 IEPOX dimer sulfate esters ( $[\text{C}_{10}\text{H}_{21}\text{O}_{10}\text{S}]^-$ ,  $m/z$  333) (Surratt et al., 2008), and 2-MG sulfate  
17 ester ( $[\text{C}_4\text{H}_7\text{O}_7\text{S}]^-$ ,  $m/z$  199) (Lin et al., 2013b), were analyzed by UPLC/DAD-ESI-HR-  
18 QTOFMS. The UPLC/DAD-ESI-HR-QTOFMS was operated in both negative and positive  
19 ion modes; however, only the negative ion mode data is presented here since the positive ion  
20 mode data were recently described in Lin et al. (2014). Filter extract residues were  
21 reconstituted with 150  $\mu$ L of a 50:50 (v/v) solvent mixture of methanol (LC-MS Chromasolv-  
22 grade, Sigma Aldrich) and laboratory Milli-q water and a 5  $\mu$ L aliquot of each sample was  
23 eluted with solvent of the same composition. IEPOX-derived sulfate esters (2-methyltetrol  
24 sulfate esters) were quantified using an authentic standard synthesized at UNC, while sodium

1 propyl sulfate was used to quantify the remaining isoprene-derived organosulfates. The 2-  
2 methyltetrol sulfate ester standards were obtained and used as tetrabutylammonium salts. The  
3 synthetic procedure will be described in a forthcoming publication. The  $^1\text{H}$  NMR trace (Fig.  
4 S14) shows the purity of the sulfate ester mixture is  $>99\%$ . The response factor of the  
5 authentic sulfate ester standards from several analyses is a factor of  $2.25\pm 0.13$  lower than that  
6 of sodium propyl sulfate used in previous field studies (Lin et al., 2013a), suggesting that the  
7 IEPOX organosulfates likely make a contribution to mass concentration higher by a factor of  
8  $\sim 2.3$  than previously estimated at field sites. Table 1 summarized data for isoprene-derived  
9 SOA tracers quantified from 123 filter samples using the above techniques.

### 10 **2.5.3 Filter Analysis of WSOC and OC Constituents**

11 For analysis of water-soluble organic compound (WSOC) concentrations, additional  
12 filter punches (47 mm) were placed in pre-cleaned glass vials and extracted with 30 or 40 mL  
13 ultra pure water by sonication for 40 min at 1 kHz. Extracts were filtered through a syringe  
14 filter (0.45  $\mu\text{m}$ , GE Healthcare UK Limited, UK) to remove insoluble particles. Samples were  
15 extracted batch-wise, with each batch containing 12-21 ambient samples, one lab blank, and  
16 one sample spiked with  $1000\ \mu\text{gC L}^{-1}$ . Total organic carbon (TOC) was analyzed using a  
17 5310 C TOC Analyzer and 900 Inorganic Carbon Remover (ICR). The instrument was  
18 calibrated by single-point calibration with  $1000\ \mu\text{gC L}^{-1}$  of potassium hydrogen phthalate  
19 (KHP) and sodium carbonate. The calibration was verified with  $1000\ \mu\text{gC L}^{-1}$  of sucrose, and  
20 checked daily with a  $1000\ \mu\text{gC L}^{-1}$  of KHP standard. Standards and samples were run in  
21 triplicate; the first data point was rejected and the following two averaged.

22 Total OC and elemental carbon (EC) measurements from filter samples were  
23 conducted at the National Exposure Research Laboratory, U.S. Environmental Protection  
24 Agency, at Research Triangle Park, NC. A  $1.5\ \text{cm}^2$  punch was taken from each filter for

1 OC/EC analysis using the thermal-optical method (Birch and Cary, 1996) on a Sunset  
2 Laboratory (Tigard, OR) OC/EC instrument. Table S4 provides temperature and purge gas  
3 settings for the method. The instrument was calibrated internally using methane gas and the  
4 calibration was verified with sucrose solution at four mass concentrations.

## 5 **2.6 Estimations of Aerosol pH and IEPOX-Derived SOA Tracers**

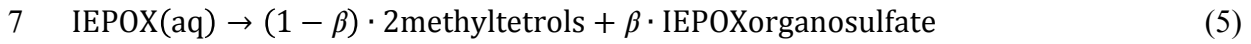
6 The thermodynamic model, ISORROPIA-II (Fountoukis and Nenes, 2007, Nenes et  
7 al., 1999), is used to estimate aerosol pH. Inputs for the model include aerosol-phase sulfate,  
8 nitrate, and ammonium in  $\mu\text{mol m}^{-3}$ , measured by the ACSM under ambient conditions; RH  
9 and temperature obtained from National Park Service (NPS); and gas-phase ammonia  
10 obtained from Ammonia Monitoring Network (AMoN; TN01/Great Smoky Mountains  
11 National Park – Look Rock). ISORROPIA-II predicted particle hydronium ion concentration  
12 per volume of air ( $H_{\text{air}}^+$ ,  $\mu\text{g m}^{-3}$ ), aerosol water (LWC,  $\mu\text{g m}^{-3}$ ), and aerosol aqueous phase  
13 mass concentration ( $\mu\text{g m}^{-3}$ ). Aerosol pH is calculated by the following equation:

$$14 \quad pH = -\log_{10} a_{H^+} = -\log_{10} \left( \frac{H_{\text{air}}^+}{LMASS} \times \rho_{\text{aer}} \times 1000 \right) \quad (4)$$

15 where  $a_{H^+}$  is  $H^+$  activity in aqueous phase ( $\text{mol L}^{-1}$ ),  $LMASS$  is the total liquid-phase aerosol  
16 mass ( $\mu\text{g m}^{-3}$ ) and  $\rho_{\text{aer}}$  is aerosol density ( $\text{g cm}^{-3}$ ). The ability of ISORROPIA to capture pH,  
17 LWC and gas-to-particle partitioning of inorganic volatiles (e.g.,  $\text{NH}_3$ ,  $\text{HNO}_3$ ,  $\text{HCl}$ ) has been  
18 the focus of other studies (Fountoukis et al., 2009, RW.ERROR - Unable to find  
19 reference:433) and is not further discussed here.

20 IEPOX-derived SOA tracers are estimated using simpleGAMMA (Woo and McNeill,  
21 2015). It is a reduced version of GAMMA (Gas Aerosol Model for Mechanism Analysis), the  
22 detailed photochemical box model of aqueous aerosol SOA (aqSOA) formation developed by  
23 McNeill and coworkers (McNeill et al., 2012). GAMMA and simpleGAMMA represent

1 aqSOA formation in terms of bulk aqueous uptake followed by aqueous-phase reaction  
 2 (Schwartz, 1986). For this study, we utilized only the aqueous aerosol-phase chemistry of  
 3 IEPOX to predict IEPOX-derived SOA constituents. We applied the Henry's law constant of  
 4  $3 \times 10^7 \text{ M atm}^{-1}$  for IEPOX partitioning based on measurements by Nguyen et al. (2014) on  
 5 deliquesced NaCl particles. Estimation of 2-methyltetrols and IEPOX-derived organosulfate  
 6 masses in the aqueous phase was based on the Eddingsaas et al. (2010) mechanism:



8 where  $\beta$  is a branching ratio between 2-methyltetrols and IEPOX-derived organosulfate  
 9 concentration. We applied  $\beta = 0.4$  based on the observation of Eddingsaas et al. (2010) for the  
 10 most concentrated bulk solution they studied. The rate constant for reaction (5) ( $ka$ ) is a  
 11 function of  $a_{H^+}$  and nucleophile concentrations (Eddingsaas et al., 2010), modified to include  
 12 the possible protonation of IEPOX(aq) by ammonium (Nguyen et al., 2014):

$$13 ka = k_{H^+} a_{H^+} + k_{SO_4^{2-}} [SO_4^{2-}] a_{H^+} + k_{HSO_4^-} [HSO_4^-] + k_{NH_4^+} [NH_4^+] \quad (6)$$

14 Here,  $k_{H^+} = 5 \times 10^{-2} \text{ s}^{-1}$ ,  $k_{SO_4^{2-}} = 2 \times 10^{-4} \text{ M}^{-1} \text{ s}^{-1}$ , and  $k_{HSO_4^-} = 7.3 \times 10^{-4} \text{ M}^{-1} \text{ s}^{-1}$ . The  
 15 ammonium rate constant,  $k_{NH_4^+}$ , was calculated using GAMMA and the results of the  
 16 chamber study of Nguyen et al. (2014) to be  $1.7 \times 10^{-5} \text{ M}^{-1} \text{ s}^{-1}$ .

17 IEPOX uptake and formation of 2-methyltetrols and IEPOX-derived organosulfate  
 18 was computed using simpleGAMMA with inputs of  $SO_4^{2-}$ ,  $HSO_4^-$ ,  $NH_4^+$ , LWC,  $a_{H^+}$   
 19 concentrations ( $\text{mol L}^{-1}$ ), and aerosol pH estimated by ISORROPIA-II simulation of field  
 20 conditions, ambient temperature and RH, aerosol surface area ( $\text{cm}^2 \text{ cm}^{-3}$ ) obtained from  
 21 SEMS-MCPC measurements, and IEPOX concentration ( $\text{mol cm}^{-3}$ ) from acetate CIMS  
 22 (Section 2.4). Masses of SOA tracers formed over 12 hours are compared with measurements  
 23 in Section 3.4.2.

## 1   **3   Results and Discussion**

### 2   **3.1   Fine Aerosol Component Mass Concentrations**

3           Chemical measurements of fine aerosol made by the ACSM and collocated  
4 instruments are presented in Fig. 1. The ACSM measured a campaign average  $7.6 \pm 4.7 \mu\text{g m}^{-3}$   
5 of NR-PM<sub>1</sub>, which is predominantly organic aerosol (64.1%). Sulfate aerosol (24.3%) is the  
6 most dominant inorganic aerosol component, followed by ammonium (7.7%), nitrate (3.8%),  
7 and chloride (0.1%). The NR-PM<sub>1</sub> mass measured at the site shows strong association ( $r^2 =$   
8 0.89) with the SEMS-MCPC PM<sub>1</sub> mass measurements (Figs. 1d and S3).

9           Moderate correlations, depicted in Fig. S15 were observed between ACSM OM and  
10 filter OC and WSOC ( $r^2 = 0.54, 0.39$ , respectively) as well as between filter OC and WSOC  
11 measurements ( $r^2 = 0.36$ ), suggesting that fractions of OM and OC at LRK site are water-  
12 soluble as previously observed (Turpin and Lim, 2001). This water-soluble fraction may be  
13 associated with high isoprene emissions in this area (Zhang et al., 2012a). Lewis et al. (2004)  
14 reported that 56%-80% of total carbon in PM<sub>2.5</sub> samples collected during summer in  
15 Nashville, TN, was non-fossil carbon, supporting the importance of biogenic SOA in the  
16 southeastern U.S. during summer. It is potentially possible that some fraction of this non-  
17 fossil carbon is associated to biomass burning (Ke et al., 2007). A more recent study found  
18 that non-fossil carbon accounts for 50% of carbon at two urban sites and 70%–100% of  
19 carbon at 10 near-urban or remote sites in the U.S. (Schichtel et al., 2008). In summer 2001,  
20 the fraction of non-fossil carbon was reported to vary from 66-80% of total carbon at the  
21 LRK, TN site, suggesting the importance of photochemical oxidation of biogenic VOCs  
22 (Tanner et al., 2004). The slope of the linear regression analysis on Fig. S15a indicates an  
23 OM:OC ratio of 2.34 and OM:WSOC ratio of 2.19. Using the Aiken et al. (2008)  
24 parameterization approach, we found an average ( $\pm 1\text{-}\sigma$ ) OM:OC ratio of 2.14 ( $\pm 0.18$ ). The

1 LRK OM:OC ratios obtained from measurements and parameterization are consistent with a  
2 previous study at Look Rock (2.1) (Turpin and Lim, 2001), but higher than those measured at  
3 Centerville, AL (1.77) (Sun et al., 2011), probably ascribable to different atmospheric aerosol  
4 properties at the two sites.

5 Elemental analyses of ACSM unit-mass resolution data using the Aiken et al. (2008)  
6 parameterization results in an average O:C ratio of  $0.77 \pm 0.12$ . This is within 0.6–1 of O:C  
7 ratio previously observed in the southeastern U.S. (Centerville, AL) (Sun et al., 2011, Xu et  
8 al., 2015).

9 ACSM sulfate aerosol measurements (average of  $1.85 \pm 1.23 \mu\text{g m}^{-3}$ ) agree well ( $r^2 =$   
10  $0.67$ , slope  $1.08$ ) with the collocated sulfate measurements (Table S1), demonstrating that  
11 ACSM performed well when compared to existing air quality monitoring instruments as  
12 previously reported (Budisulistiorini et al., 2014). Low nitrate concentration is expected due  
13 to the high summer temperatures ( $15\text{--}31^\circ\text{C}$ ) and low prevailing  $\text{NO}_x$  concentrations ( $0.1\text{--}2$   
14 ppb) measured at the site. In the absence of a significant source of chloride, chloride  
15 concentrations were predictably low ( $0.01 \pm 0.01 \mu\text{g m}^{-3}$ ).

16 On average, mass concentration of BC was  $0.23 \pm 0.14 \mu\text{g m}^{-3}$  or about 3% of total  
17  $\text{PM}_{2.5}$  measured at the site. The low relative contribution was consistent during the campaign  
18 except on 11 to 12 July when there was a significant increase during few hours overnight. EC  
19 measured from filters was even lower at  $0.06 \mu\text{g m}^{-3}$  on average and was only weakly  
20 correlated ( $r^2 = 0.32$ ) with BC. Carbon monoxide (CO), another primary species measured at  
21 LRK, was also low ( $115.62 \pm 24.06$  ppb on average) throughout the campaign. A previous  
22 study found that the level of primary species increased during mid-morning when the  
23 boundary layer height reached the site, and declined later in the day as a result of dilution  
24 (Tanner et al., 2005). In contrast, secondary species such as  $\text{PM}_{2.5}$  and sulfate do not show

1 significant diurnal variability, suggesting local meteorological conditions are less influential  
2 in determining concentrations of the long-lived species (Tanner et al., 2005, Tanner et al.,  
3 2015). The overall low concentration of primary emissions at the site (Fig. S16) is consistent  
4 with minimum local and/or regional primary emissions.

### 5 **3.2 Source Apportionment of OA from the ACSM**

6 PMF analysis was conducted on the ACSM OA mass spectral data in order to resolve  
7 factors (or source profiles) without a-priori assumptions. A 3-factor solution resolved from  
8 PMF analysis, as shown in Figs. 2 and 3, was selected as the best-fit (see SI for details of  
9  $Q/Q_{exp}$ ,  $f_{peak}$ , etc.), comprised of the known LV-OOA factor (Jimenez et al., 2009, Ulbrich et  
10 al., 2009), an IEPOX-OA factor (Budisulistiorini et al., 2013, Slowik et al., 2011, Robinson et  
11 al., 2011), and a factor similar to 91Fac, a factor previously observed in areas dominated by  
12 biogenic emissions (Robinson et al., 2011, Slowik et al., 2011, Chen et al., 2014).

13 The IEPOX-OA factor resolved from our dataset is more closely correlated to sulfate  
14 measured by the ACSM ( $r^2 = 0.58$ ) than by the collocated instrument ( $r^2 = 0.31$ ) (Table S5).  
15 Correlation of gaseous IEPOX measured by acetate CIMS with the IEPOX-OA factor is low  
16 ( $r^2 = 0.24$ ), which may be a consequence of time gap from IEPOX uptake onto sulfate aerosol  
17 process which can take up ~5 hours in the presence of aqueous, highly acidic aerosol ( $\text{pH} \leq 1$ )  
18 (Gaston et al., 2014). The time gap between formation of gaseous IEPOX and IEPOX-OA  
19 factor could be wider due to ISOPOOH, which lifetime to OH is 3 – 5 hours (Paulot et al.,  
20 2009), interference on IEPOX signal measured by acetate acetate CIMS. Importantly, the  
21 IEPOX-OA factor correlates strongly with 2-methyltetrols ( $r^2 = 0.80$ ), IEPOX-derived  
22 organosulfates ( $r^2 = 0.81$ ), C<sub>5</sub>-alkene triols ( $r^2 = 0.75$ ), and dimers of organosulfates ( $r^2 =$   
23 0.73) (Table 2), giving an overall  $r^2$  of 0.83 with sum of IEPOX-derived SOA tracers  
24 measured by offline techniques. The high correlation provides strong evidence that IEPOX

1 chemistry gives rise to the PMF factor we have designated as the IEPOX-OA factor. The  
2 contribution of this factor to total OM is 32%, which is strikingly consistent with the  
3 contribution of the factor designated as the IEPOX-OA factor in the PMF analysis of fine  
4 organic aerosol collected in downtown Atlanta, GA (Budisulistiorini et al., 2013) and across  
5 other sites in this region (Xu et al., 2015). IEPOX-OA was not only formed on site but could  
6 also be transported from surrounding forested and isoprene-rich areas. The reactive-uptake of  
7 IEPOX is influenced by aerosol sulfate (Lin et al., 2012) that is not formed on site, might  
8 explain the lack of significant diurnal variation (Fig. 3) of the IEPOX-OA factor at LRK.  
9 WSOC shows fair correlation with some IEPOX-OA tracers ( $r^2 = 0.3\text{--}0.4$ ; Table S6) and  
10 IEPOX-OA factor ( $r^2 = 0.37$ ; Table S5) the nature of which will be discussed in more detail  
11 below.

12 The LV-OOA factor contributes 50% of OM (Fig. 3). The average  $f_{44} = 0.22$  is  
13 comparable to that of the standard LV-OOA profile (Ng et al., 2011), suggesting it is an  
14 oxidized (aged) aerosol. The LV-OOA correlated well with nitrate ( $r^2 = 0.62$ ) but more  
15 weakly with sulfate ( $r^2 = 0.39$ ) (Table S5). Correlation with nitrate as well as the high level of  
16 oxidation is consistent with the suggestion above that a fraction of OA originates from the  
17 valley. Located on a ridge top above the morning valley fog, LRK receives air masses from  
18 the valley as the boundary layer rises during the day (Tanner et al., 2005). Diurnal profile of  
19 LV-OOA observed at LRK is similar to more-oxidized OOA (MO-OOA) observed at  
20 Centerville (Xu et al., 2015), suggesting their regional sources. At LRK average mixing ratios  
21 of monoterpenes and isoprene were  $<1$  ppb and  $\sim 2$  ppb (Fig. 4), respectively. Low  
22 anthropogenic emissions at LRK ( $<1$  ppb; Fig. S16) suggests that BVOCs could be the source  
23 of LV-OOA (50% of OA) formation. Anthropogenic emissions as well as nitrate chemistry in

1 the valley could also influence LV-OOA formation that oxidized during transport to the LRK  
2 site.

3 The 91Fac factor is characterized by a distinct ion at  $m/z$  91. At LRK, the average  $f_{44}$   
4 of 91Fac is 0.12, between the values 0.05 and 0.16 reported for standard SV-OOA and LV-  
5 OOA profiles, respectively (Ng et al., 2011), indicating that it is likely an oxygenated OA.  
6 The LRK 91Fac makes the smallest contribution to OM (18%) of the three factors resolved by  
7 PMF analysis. The 91Fac diurnal pattern shows slight increases during noon and night,  
8 suggesting that this factor might be affected by both photochemistry and nighttime chemistry.  
9 Potential sources of 91Fac is discussed in more detail in the SI (Fig. S17) and its association  
10 with biogenic SOA chemistry will be the focus of future studies.

11 A source apportionment study of organic compounds in  $PM_{2.5}$  at LRK during August  
12 2002 using the chemical mass balance (CMB) model evaluated contributions by eight primary  
13 sources, chosen as representing the major contributors to fine primary OC in the southeast  
14 U.S. Primary sources, consisting largely of wood burning, were estimated to contribute ~14%  
15 of the total OC at LRK (Ke et al., 2007).  $^{14}C$  Analysis of the LRK  $PM_{2.5}$  in the same study  
16 showed that during summer, ~84% of the OC was non-fossil carbon (Ke et al., 2007). By  
17 contrast, our current study resolved no POA by PMF analysis. However, in subsequent  
18 studies, we will investigate the influence of POA at LRK by examining the  $^{14}C$  data from  
19 filter samples.

### 20 **3.3 Identification and Quantification of Isoprene-derived SOA Tracers**

21 2-Methylglyceric acid, 2-methyltetrols,  $C_5$ -alkene triols and IEPOX-derived  
22 organosulfates were detected in most filter samples (Table 1). Among all observed SOA  
23 tracers, 2-C-methylerythritol and 2-methylbut-3-ene-1,2,4-triol were the most abundant

1 species identified by GC/EI-MS, contributing ~24% (120.7 ng m<sup>-3</sup> on average) and ~20%  
2 (98.8 ng m<sup>-3</sup> on average), respectively, of total quantified mass, while isomeric IEPOX-  
3 derived organosulfates accounted for ~34% (169.5 ng m<sup>-3</sup> on average) of the mass detected by  
4 UPLC/DAD-ESI-HR-QTOFMS. Concentrations of the isomeric 3-MeTHF-3,4-diols were  
5 lower ( $\leq 18.8$  ng m<sup>-3</sup>), often at or below detection limits. Gaseous IEPOX was on average 1  
6 ppb (maximum 5.8 ppb) significantly higher than gaseous MAE at  $2.8 \times 10^{-3}$  ppb on average  
7 (maximum 0.02 ppb). This explains the abundance of IEPOX-derived SOA tracers compared  
8 to MAE-derived tracers. It should be noted that IEPOX quantified here includes the  
9 interference of ISOPOOH on its signal; however, the overall measured IEPOX signal is still  
10 substantially higher than the MAE signal, even if we assume IEPOX only contributes to 1 –  
11 10% of the *m/z* 177 intensity.

12 In sum, IEPOX- and MAE-derived tracers contributed 96.6% and 3.4%, respectively,  
13 of total isoprene-derived SOA mass quantified from filter samples. This observation is  
14 consistent with a previous field study in Yorkville, GA, which reported the summed IEPOX-  
15 derived SOA tracers comprised 97.5% of the quantified isoprene-derived SOA mass (Lin et  
16 al., 2013a). Total IEPOX-derived tracers masses quantified from filter samples were on  
17 average 26.3% (maximum 48.5%) of the IEPOX-OA factor mass resolved by PMF. This is  
18 consistent with a recent laboratory study of isoprene photooxidation under high HO<sub>2</sub>  
19 conditions that suggested IEPOX isomers contributed about 50% of SOA mass formed (Liu et  
20 al., 2014).

21 Masses of IEPOX- and MAE-derived SOA tracers were fairly correlated ( $r^2 = 0.37$   
22 and 0.29, respectively) with WSOC (Fig. S15c). Around 26% of the WSOC mass might be  
23 explained by IEPOX-derived SOA tracer masses, which consist predominantly of 2-  
24 methyltetrols, C<sub>5</sub>-alkene triols, and IEPOX-derived organosulfates. The tetrols and triols are

1 hydrophilic compounds owing to the OH groups, and the organosulfates are ionic polar  
2 compounds (Gómez-González et al., 2008).

3 An interesting and potentially important observation is that oligomeric IEPOX-derived  
4 humic-like substances (HULIS) have been reported in both reactive uptake experiments onto  
5 acidified sulfate seed aerosol and in ambient fine aerosol from the LRK and Centerville sites  
6 during the SOAS campaign (Lin et al., 2014). The HULIS is a mixture of hydroxylated,  
7 sulfated as well as highly unsaturated, light-absorbing components which may partition  
8 between WSOC and water insoluble organic carbon (WISC) fractions (Lin et al., 2014). This  
9 finding might also in part explain the moderate correlation between WSOC and the IEPOX-  
10 OA factor. However, HULIS has not been quantified here due to the lack of authentic  
11 standards, but will likely help to close the IEPOX-OA mass budget once appropriate  
12 standards are developed and applied. As quantified by ACSM, summed isoprene-derived  
13 SOA tracers on average accounted for  $0.5 \mu\text{g m}^{-3}$  or 9.4% (up to  $4.4 \mu\text{g m}^{-3}$  or 28.1%) of the  
14 average organic aerosol mass of  $5.1 \mu\text{g m}^{-3}$  (maximum  $15.3 \mu\text{g m}^{-3}$ ) during the campaign. This  
15 contribution is somewhat lower than reported at a different rural site in the southeast U.S.  
16 (13.6% - 19.4%) (Lin et al., 2013a) but higher than reported at a forested site in central  
17 Europe (6.8%) (Kourtchev et al., 2009) and a rural site in south China (1.6%) (Ding et al.,  
18 2012). It should be noted that in all previous studies sulfate esters of 2-methyltetrol were  
19 quantified by surrogate standard structurally unrelated to the target analytes (i.e., sodium  
20 propyl sulfate). While in current study, a mixture of authentic 2-methyltetrol sulfate esters  
21 was used as a standard for quantifying IEPOX-derived organosulfates. The use of structurally  
22 unrelated surrogate standards may account in part for discrepancies between this and previous  
23 studies in which total isoprene SOA mass may have been underestimated as a result of higher  
24 instrument response to surrogates and/or lower recovery in sample preparation. These

1 possibilities warrant further investigation using the same analytical protocols and comparison  
2 of instrumental responses to authentic and surrogate standards.

### 3 **3.4 Influence of Anthropogenic Emissions on Isoprene-Derived SOA Formation at** 4 **Look Rock**

#### 5 **3.4.1 Effects of aerosol acidity and nitrogen-containing species**

6 The time series of aerosol pH estimated by ISORROPIA-II overlaid on the time series  
7 of the IEPOX-OA factor and IEPOX- and MAE-derived SOA tracers (Fig. 5a, Tables S5-S6)  
8 suggests that local aerosol acidity is not correlated with these measured variables. The  
9 correlation coefficients of the IEPOX-OA factor with ISORROPIA-II estimated pH and LWC  
10 bears out this conclusion ( $r^2 \sim 0$ ; Table S5). These results are consistent with recent  
11 measurements reported by Xu et al. (2015) across several sites in the southeastern U.S.  
12 Aerosol acidity can be expected to change during transport and aging. Further complicating  
13 factors may be viscosity or morphology changes of the aerosol as IEPOX is taken up by  
14 heterogeneous reaction, and thus, slowing of uptake kinetics as the aerosol surface is coated  
15 with a hydrophobic organic layer (Gaston et al., 2014). Additionally, liquid-liquid phase  
16 separation is likely to occur in the atmosphere due to changes of relative humidity that affect  
17 particles water content (You et al., 2012). Moreover, the effects of aerosol viscosity and  
18 morphology on IEPOX uptake is not well understood and warrant further study using aerosol  
19 of complex mixtures and of atmospheric relevance. Interpretation of the apparent lack of  
20 relationship between SOA and local aerosol acidity suggests that aerosol acidity is likely not  
21 the limiting factor in isoprene SOA formation at this site, especially since aerosol was  
22 consistently acidic during SOAS. The IEPOX-OA factor is moderately correlated with aerosol  
23 sulfate measured by ACSM ( $r^2 = 0.58$ ), while IEPOX- and MAE-derived SOA tracers are less

1 correlated ( $r^2 \sim 0.4$ ) (Fig. 5b). Correlation between sulfate and IEPOX-OA factor is consistent  
2 with recent measurements by Xu et al. (2015), and suggests the need for aerosol surface area  
3 due to acidic sulfate for these heterogeneous reactions to occur leading to IEPOX-OA  
4 formation.

5 Correlation of IEPOX-OA and isoprene-derived SOA tracers with  $\text{NO}_x$ ,  $\text{NO}_y$ , and  
6 reservoir species ( $\text{NO}_z = \text{NO}_y - \text{NO}_x$ ) was also examined. None of the nitrogen species  
7 showed significant association with either the IEPOX-OA factor ( $r^2 < 0.1$ ; Table S5) or the  
8 IEPOX-derived SOA tracers ( $r^2 < 0.3$ ; Table S5). Absence of correlations suggest that: (1) the  
9 formation of isoprene SOA primarily through the low-NO pathway of isoprene  
10 photooxidation (Paulot et al., 2009, Surratt et al., 2010), (2) the isoprene oxidation did not  
11 happen locally, and (3) the gas-phase isoprene oxidation is not yet fully understood.  
12 Correlation plot of  $\text{NO}_y$ , a measure of total reactive nitrogen species including MPAN, with  
13 summed MAE tracers is shown in Fig. 5c and correlation values of  $\text{NO}_x$  with individual  
14 compounds are given in Table S6. Besides being derived solely from the hydrolysis of MAE,  
15 2-MG is also proposed to be the hydrolysis product of hydroxymethyl-methyl- $\alpha$ -lactone  
16 (HMML) (Nguyen et al., 2015) and fair correlation between  $\text{NO}_y$  and 2-MG ( $r^2 = 0.38$ ) is  
17 consistent with this hypothesis. The correlation of the high- $\text{NO}_x$  isoprene SOA tracers (2-MG  
18 and its corresponding organosulfate) with  $\text{NO}_y$  is suggesting that other pathways like the  
19 uptake and hydrolysis of MAE could be a source, especially since the further oxidation of  
20 MACR has been shown to yield MAE directly (Lin et al., 2013b). The observation that  
21 neither the summed MAE/HMML-derived tracers nor 2-MG correlated with  $\text{NO}_x$ , is  
22 consistent with the hypothesis that MAE/HMML is formed in urban areas upwind and  
23 transported to the sampling site. Furthermore, it suggests that likely both HMML and MAE  
24 could be sources of these tracers.

1 In addition to the pattern of daily up-slope transport of air from the valley, air mass  
2 back-trajectory during high IEPOX-derived SOA episodes (Fig. S18) indicated that air masses  
3 also originated west of LRK, in the direction of the urban areas of Knoxville and Nashville,  
4 TN. Yet further west of the LRK site are the Missouri Ozarks, a large source of isoprene  
5 emissions (referred to as the “isoprene volcano”) (Guenther et al., 2006). During summer,  
6 isoprene emitted in the Ozarks could mix with anthropogenic emissions from Knoxville and  
7 Nashville, undergoing atmospheric processing during transport. As a consequence, long  
8 distance transport and accompanying oxidative processing may make a contribution to the  
9 IEPOX SOA loading at LRK. During low IEPOX-derived SOA periods (Fig. S19) air masses  
10 originated predominantly from the south and southwest, which are densely forested, rural  
11 areas.

### 12 **3.4.2 Box Modeling Supports the Impact of Aqueous Acidic Aerosol on IEPOX-** 13 **Derived SOA**

14 The IEPOX-derived SOA tracers (2-methyltetrols and IEPOX-derived organosulfate)  
15 predicted using simpleGAMMA, taking the locally measured IEPOX and aerosol parameters  
16 as inputs, show good correlation ( $r^2 = 0.5\text{--}0.7$ ) with the tracers quantified from filter samples  
17 (Table 3, Fig. S20). Slopes of the scatterplots show that the model overestimated the 2-  
18 methyltetrols and IEPOX-derived organosulfates by factors of 6.3 and 7.5, respectively.  
19 simpleGAMMA calculates Henry’s Law gas-aqueous equilibration at each time step and  
20 decouples the subsequent aqueous-phase chemistry of IEPOX from dissolution (McNeill et  
21 al., 2012). In this study, we assumed an effective Henry’s law constant,  $H^*$ , of  $3 \times 10^7 \text{ M atm}^{-1}$   
22 for IEPOX, following the recent laboratory measurements of Nguyen et al. (2014), whereas  
23 previous studies assumed values which ranged one order of magnitude higher ( $1.3 \times 10^8 \text{ M}$   
24  $\text{atm}^{-1}$  (Eddingsaas et al., 2010)) or lower ( $2.7 \times 10^6 \text{ M atm}^{-1}$  (Pye et al., 2013)). Replacing the

1 H\* with that of Pye et al. (2013), the model underestimated the 2-methyltetrols and IEPOX-  
2 derived organosulfates by 56% and 43%, respectively. Decreasing the H\* by one order of  
3 magnitude yielded a factor of ~10 decrease in the predicted IEPOX SOA tracers mass, which  
4 is consistent with Pye et al. (2013) observation in sensitivity studies that a factor of 7 increase  
5 in H\* yielded a factor of ~5 increase in predicted IEPOX SOA yield. Similarly, summed  
6 masses of the modeled SOA tracers (Fig. 6) yielded a 141% ( $r^2 = 0.62$ ) overestimate of the  
7 IEPOX-OA factor, whereas summed SOA tracers modeled by assuming H\* of one order of  
8 magnitude lower yielded an 89% underestimate of the IEPOX-OA factor ( $r^2 = 0.62$ ).  
9 simpleGAMMA predicts only a subset of IEPOX-derived SOA tracers, thus underestimation  
10 of the IEPOX-OA factor is expected.

11 In addition to the uncertainty in the H\* parameter, several other factors may also  
12 contribute to mass disagreement between the tracer estimated by simpleGAMMA and the  
13 field data. The box model simulations took locally measured IEPOX and aerosol parameters  
14 as inputs, and simulated 12 hours of reactive processing, rather than simulating uptake,  
15 reaction, and transport along a trajectory initiating in the valley. The locally measured IEPOX  
16 signal is noted above to have interference from ISOPOOH, thus the model outputs likely  
17 overestimate the measurements. Examination of IEPOX input variability to simpleGAMMA  
18 tracers estimation will be reported in a future study. Additionally, C<sub>5</sub>-alkene triols, the third  
19 largest contributor to the IEPOX-derived SOA tracers, and oligomeric HULIS are not  
20 included in the simpleGAMMA model estimation. Neglect of the C<sub>5</sub>-alkene triols and  
21 oligomers as well as yet unknown IEPOX-derived SOA formation pathways by this model  
22 could contribute to inaccuracy in estimation of the mass contribution of 2-methyltetrols and  
23 IEPOX-derived organosulfates to the total amount of IEPOX-derived SOA tracers and reduce  
24 the correlation. Finally, oxidative aging of IEPOX SOA tracers is not included in

1 simpleGAMMA at this time due to current lack of availability of kinetic and mechanistic data.  
2 Overall, although mass disagreement persists, good correlation between model and field  
3 measurements of tracers suggest that the uptake mechanism of IEPOX is consistent with acid-  
4 catalyzed mechanism proposed from kinetic (Eddingsaas et al., 2010, Pye et al., 2013) and  
5 laboratory studies (Lin et al., 2012, Nguyen et al., 2014).

#### 6 **4 Conclusions**

7 Offline chemical analysis of PM<sub>2.5</sub> samples collected from LRK, TN, during the 2013  
8 SOAS campaign show a substantial contribution by IEPOX-derived SOA tracers to the total  
9 OA mass (~9% on average, up to 28%). A larger contribution (32%) to total OA mass is  
10 estimated by PMF analysis of the real-time ACSM OA mass spectrometric data. Overall, the  
11 importance of IEPOX heterogeneous chemistry in this region is clearly demonstrable. No  
12 association was observed between the gas-phase constituents NO and NO<sub>2</sub> and the IEPOX-  
13 derived SOA tracers or the IEPOX-OA factor suggesting that IEPOX-derived SOA formed  
14 upwind or distant from the sampling site. Moderate association between NO<sub>y</sub> and MACR-  
15 derived SOA tracers was observed, consistent with the proposed involvement of oxidizing  
16 nitrogen compounds in MACR-derived SOA formation (Lin et al., 2013b, Nguyen et al.,  
17 2015). Particle-phase sulfate is fairly correlated ( $r^2 = 0.3-0.4$ ) with both MACR- and IEPOX-  
18 derived SOA tracers, and more strongly correlated ( $r^2 \sim 0.6$ ) with the IEPOX-OA factor,  
19 overall suggesting that sulfate plays an important role in isoprene SOA formation. However,  
20 this association requires further analysis, in light of the proposed formation of IEPOX-derived  
21 SOA during transport to LRK from an upwind or down-slope origin. Several explanations  
22 may be proposed for the lack of a strong association between isoprene-derived SOA mass and  
23 particle acidity: 1) isoprene-derived SOA is not strongly limited by levels of predicted aerosol  
24 acidity and LWC even though these are in the favored ranges ( $\text{pH} < 2$ ) to promote sufficient

1 SOA production based on recent laboratory kinetic studies (Gaston et al., 2014, Riedel et al.,  
2 2015) and thus, other potentially unknown controlling factors in this region might need to be  
3 considered; 2) no strong correlation exists between SOA mass and local aerosol acidity which  
4 estimation is challenging due to changes in particle composition and characteristics during  
5 reactive uptake and 3) several key inter-related variables (LWC, aerosol surface area and  
6 aerosol acidity) control SOA yield and thus the correlation of aerosol acidity and SOA yield  
7 will be difficult to deconvolute from complex field data until modeling can better constrain  
8 these effects. Consistent with the suggestion that IEPOX-derived SOA forms during transport  
9 from distant locations, air mass back-trajectory indicated that westerly flow from potential  
10 sources of oxidation products where biogenic and anthropogenic emissions can mix, are likely  
11 related to episodes of high levels of IEPOX-derived SOA measured at LRK. In contrast, when  
12 air masses originated mainly from forested and rural areas to the south and southeast of the  
13 site, high levels of IEPOX-derived SOA mass were not observed. Good correlation between  
14 SOA model outputs and field measurements suggests that gaps remain in our knowledge of  
15 isoprene-derived SOA formation. Laboratory studies are needed to reduce the uncertainty in  
16 the effective Henry's Law constant,  $H^*$ , for IEPOX. Additional studies are needed to further  
17 quantify the condensed-phase mechanism and kinetics of SOA formation via the IEPOX  
18 pathway so that it may be represented in more detail in models. Notwithstanding, initial  
19 modeling results allow critical insight into how more explicit treatment of the reactions  
20 between anthropogenic pollutants and isoprene oxidation products may be incorporated into  
21 models of SOA formation. Importantly, by inclusion of explicit IEPOX- and MAE-derived  
22 SOA formation pathways in a model, Pye et al. (2013) recently demonstrated that by lowering  
23  $SO_x$  emissions in the eastern U.S. by 25% could lower IEPOX- and MAE-derived SOA  
24 formation 35 to 40%. Future studies should attempt to improve model predictions of IEPOX-

1 derived SOA formation and systematically examine effects of implementing stricter SO<sub>x</sub>  
2 controls in this region.

### 3 **Acknowledgements**

4 This work was funded by the U.S. Environmental Protection Agency (EPA) through grant  
5 number 835404. The contents of this publication are solely the responsibility of the authors  
6 and do not necessarily represent the official views of the U.S. EPA. Further, the U.S. EPA  
7 does not endorse the purchase of any commercial products or services mentioned in the  
8 publication. The U.S. EPA through its Office of Research and Development collaborated in  
9 the research described here. It has been subjected to Agency review and approved for  
10 publication, but may not necessarily reflect official Agency policy. The author would also like  
11 to thank the Electric Power Research Institute (EPRI) for their support. This study was  
12 supported in part by the National Oceanic and Atmospheric Administration (NOAA) Climate  
13 Program Office's AC4 program, award # NA13OAR4310064. We thank Bill Hicks of the  
14 Tennessee Valley Authority (TVA) for his assistance in collecting the collocated monitoring  
15 data at the LRK site. S. H. Budisulistiorini was supported by a Fulbright Presidential  
16 Fellowship (2010–2013) for attending the University of North Carolina at Chapel Hill and the  
17 UNC Graduate School Off-Campus Dissertation Research Fellowship, as well as partial  
18 appointment to the Internship/Research Participation Program at the Office of Research and  
19 Development, U.S. EPA, administered by the Oak Ridge Institute for Science and Education  
20 through an interagency agreement between the U.S. Department of Energy and EPA. M. Neff  
21 and E. A. Stone were supported by US EPA Science to Achieve Results (STAR) program  
22 grant number 835401. The authors thank Lynn Russell, Timothy Bertram and Christopher  
23 Cappa as well as their respective groups for their collaboration during the SOAS campaign at  
24 LRK. The authors thank Louisa Emmons for her assistance with forecasts made available

1 during the SOAS campaign. The authors thank John Offenberg for providing access to Sunset  
2 OC/EC analysis instrument. The authors also thank Tianqu Cui for his assistance in helping  
3 deploy instrumentation from the UNC group, and Wendy Marth and Theran Riedel for their  
4 assistance in helping calibrate the acetate CIMS. We would like to thank Annmarie Carlton,  
5 Joost deGouw, Jose Jimenez, and Allen Goldstein for helping to organize the SOAS campaign  
6 and coordinating communication between ground sites.

## 7 **References**

- 8 Aiken, A. C., DeCarlo, P.F., Kroll, J.H., Worsnop, D.R., Huffman, J.A., Docherty, K.S., Ulbrich,  
9 I.M., Mohr, C., Kimmel, J.R., Sueper, D., Sun, Y., Zhang, Q., Trimborn, A., Northway, M.,  
10 Ziemann, P.J., Canagaratna, M.R., Onasch, T.B., Alfarra, M.R., Prevot, A.S.H., Dommen, J.,  
11 Duplissy, J., Metzger, A., Baltensperger, U. and Jimenez, J.L.: O/C and OM/OC Ratios of  
12 Primary, Secondary, and Ambient Organic Aerosols with High-Resolution Time-of-Flight  
13 Aerosol Mass Spectrometry, *Environ. Sci. Technol.*, 42, 4478-4485, doi:10.1021/es703009q,  
14 2008.
- 15 Bates, K. H., Crounse, J.D., St. Clair, J.M., Bennett, N.B., Nguyen, T.B., Seinfeld, J.H., Stoltz, B.M.  
16 and Wennberg, P.O.: Gas Phase Production and Loss of Isoprene Epoxydiols, *J. Phys. Chem. A*,  
17 118, 1237-1246, doi:10.1021/jp4107958, 2014.
- 18 Bertram, T. H., Kimmel, J.R., Crisp, T.A., Ryder, O.S., Yatavelli, R.L.N., Thornton, J.A., Cubison,  
19 M.J., Gonin, M. and Worsnop, D.R.: A field-deployable, chemical ionization time-of-flight mass  
20 spectrometer, *Atmos. Meas. Tech.*, 4, 1471-1479, doi:10.5194/amt-4-1471-2011, 2011.
- 21 Birch, M. E. and Cary, R.A.: Elemental carbon-based method for occupational monitoring of  
22 particulate diesel exhaust: methodology and exposure issues, *Analyst*, 121, 1183-1190,  
23 doi:10.1039/AN9962101183", 1996.
- 24 Budisulistiorini, S. H., Canagaratna, M.R., Croteau, P.L., Baumann, K., Edgerton, E.S., Kollman,  
25 M.S., Ng, N.L., Verma, V., Shaw, S.L., Knipping, E.M., Worsnop, D.R., Jayne, J.T., Weber, R.J.  
26 and Surratt, J.D.: Intercomparison of an Aerosol Chemical Speciation Monitor (ACSM) with  
27 ambient fine aerosol measurements in downtown Atlanta, Georgia, *Atmos. Meas. Tech.*, 7, 1929-  
28 1941, doi:10.5194/amt-7-1929-2014, 2014.
- 29 Budisulistiorini, S. H., Canagaratna, M.R., Croteau, P.L., Marth, W.J., Baumann, K., Edgerton, E.S.,  
30 Shaw, S.L., Knipping, E.M., Worsnop, D.R., Jayne, J.T., Gold, A. and Surratt, J.D.: Real-Time  
31 Continuous Characterization of Secondary Organic Aerosol Derived from Isoprene Epoxydiols in  
32 Downtown Atlanta, Georgia, Using the Aerodyne Aerosol Chemical Speciation Monitor,  
33 *Environ.Sci.Technol.*, 47, 5686-5694, doi:10.1021/es400023n, 2013.
- 34 Carlton, A. G., Bhave, P.V., Napelenok, S.L., Edney, E.O., Sarwar, G., Pinder, R.W., Pouliot, G.A.  
35 and Houyoux, M.: Model Representation of Secondary Organic Aerosol in CMAQv4.7,  
36 *Environ.Sci.Technol.*, 44, 8553-8560, doi:10.1021/es100636q, 2010.

- 1 Chen, Q., Farmer, D.K., Rizzo, L.V., Pauliquevis, T., Kuwata, M., Karl, T.G., Guenther, A., Allan,  
2 J.D., Coe, H., Andreae, M.O., Pöschl, U., Jimenez, J.L., Artaxo, P. and Martin, S.T.: Fine-mode  
3 organic mass concentrations and sources in the Amazonian wet season (AMAZE-08), *Atmos.*  
4 *Chem. Phys. Discuss.*, 14, 16151-16186, doi:10.5194/acpd-14-16151-2014, 2014.
- 5 Claeys, M., Graham, B., Vas, G., Wang, W., Vermeylen, R., Pashynska, V., Cafmeyer, J., Guyon, P.,  
6 Andreae, M.O., Artaxo, P. and Maenhaut, W.: Formation of Secondary Organic Aerosols  
7 Through Photooxidation of Isoprene, *Science*, 303, 1173-1176, doi:10.1126/science.1092805,  
8 2004.
- 9 Cross, E. S., Slowik, J.G., Davidovits, P., Allan, J.D., Worsnop, D.R., Jayne, J.T., Lewis, D.K.,  
10 Canagaratna, M. and Onasch, T.B.: Laboratory and Ambient Particle Density Determinations  
11 using Light Scattering in Conjunction with Aerosol Mass Spectrometry, *Aerosol Sci. Technol.*,  
12 41, 343-359, doi:10.1080/02786820701199736, 2007.
- 13 Ding, X., Wang, X., Gao, B., Fu, X., He, Q., Zhao, X., Yu, J. and Zheng, M.: Tracer-based estimation  
14 of secondary organic carbon in the Pearl River Delta, south China, *J. Geophys. Res.*, 117, -  
15 D05313, doi:10.1029/2011JD016596, 2012.
- 16 Dockery, D. W., Pope, C.A., Xu, X., Spengler, J.D., Ware, J.H., Fay, M.E., Ferris, B.G. and Speizer,  
17 F.E.: An Association between Air Pollution and Mortality in Six U.S. Cities, *N.Engl.J.Med.*, 329,  
18 1753-1759, doi:10.1056/NEJM199312093292401, 1993.
- 19 Eddingsaas, N. C., VanderVelde, D.G. and Wennberg, P.O.: Kinetics and Products of the Acid-  
20 Catalyzed Ring-Opening of Atmospherically Relevant Butyl Epoxy Alcohols, *J. Phys. Chem. A*,  
21 114, 8106-8113, doi:10.1021/jp103907c, 2010.
- 22 Edney, E. O., Kleindienst, T.E., Jaoui, M., Lewandowski, M., Offenber, J.H., Wang, W. and Claeys,  
23 M.: Formation of 2-methyl tetrols and 2-methylglyceric acid in secondary organic aerosol from  
24 laboratory irradiated isoprene/NOX/SO2/air mixtures and their detection in ambient PM2.5  
25 samples collected in the eastern United States, *Atmos. Environ.*, 39, 5281-5289,  
26 doi:10.1016/j.atmosenv.2005.05.031, 2005.
- 27 Foley, K. M., Roselle, S.J., Appel, K.W., Bhave, P.V., Pleim, J.E., Otte, T.L., Mathur, R., Sarwar, G.,  
28 Young, J.O., Gilliam, R.C., Nolte, C.G., Kelly, J.T., Gilliland, A.B. and Bash, J.O.: Incremental  
29 testing of the Community Multiscale Air Quality (CMAQ) modeling system version 4.7, *Geosci.*  
30 *Model Dev.*, 3, 205-226, doi:10.5194/gmd-3-205-2010, 2010.
- 31 Fountoukis, C. and Nenes, A.: ISORROPIA II: a computationally efficient thermodynamic  
32 equilibrium model for  $K^+ - Ca^{2+} - Mg^{2+} - NH_4^+ - Na^+ - SO_4^{2-} - NO_3^- - Cl^- - H_2O$  aerosols, *Atmos. Chem.*  
33 *Phys.*, 7, 4639-4659, doi:10.5194/acp-7-4639-2007, 2007.
- 34 Fountoukis, C., Nenes, A., Sullivan, A., Weber, R., Van Reken, T., Fischer, M., Matias, E., Moya, M.,  
35 Farmer, D. and Cohen, R.C.: Thermodynamic characterization of Mexico City aerosol during  
36 MILAGRO 2006, *Atmos. Chem. Phys.*, 9, 2141-2156, doi:10.5194/acp-9-2141-2009, 2009.
- 37 Gao, S., Ng, N.L., Keywood, M., Varutbangkul, V., Bahreini, R., Nenes, A., He, J., Yoo, K.Y.,  
38 Beauchamp, J.L., Hodyss, R.P., Flagan, R.C. and Seinfeld, J.H.: Particle Phase Acidity and  
39 Oligomer Formation in Secondary Organic Aerosol, *Environ.Sci.Technol.*, 38, 6582-6589,  
40 doi:10.1021/es049125k, 2004.

- 1 Gaston, C. J., Riedel, T.P., Zhang, Z., Gold, A., Surratt, J.D. and Thornton, J.A.: Reactive Uptake of  
2 an Isoprene-Derived Epoxydiol to Submicron Aerosol Particles, *Environ.Sci.Technol.*, 48,  
3 11178-11186, doi:10.1021/es5034266, 2014.
- 4 Gómez-González, Y., Surratt, J.D., Cuyckens, F., Szmigielski, R., Vermeylen, R., Jaoui, M.,  
5 Lewandowski, M., Offenberg, J.H., Kleindienst, T.E., Edney, E.O., Blockhuys, F., Van Alsenoy,  
6 C., Maenhaut, W. and Claeys, M.: Characterization of organosulfates from the photooxidation of  
7 isoprene and unsaturated fatty acids in ambient aerosol using liquid chromatography/(-)  
8 electrospray ionization mass spectrometry, *J. Mass. Spectrom.*, 43, 371-382,  
9 doi:10.1002/jms.1329, 2008.
- 10 Graus, M., M<sup>1</sup>/<sub>4</sub>ller, M. and Hansel, A.: High resolution PTR-TOF: Quantification and formula  
11 confirmation of VOC in real time, *J.Am.Soc.Mass Spectrom.*, 21, 1037-1044,  
12 doi:10.1016/j.jasms.2010.02.006, 2010.
- 13 Guenther, A., Karl, T., Harley, P., Wiedinmyer, C., Palmer, P.I. and Geron, C.: Estimates of global  
14 terrestrial isoprene emissions using MEGAN (Model of Emissions of Gases and Aerosols from  
15 Nature), *Atmos. Chem. Phys.*, 6, 3181-3210, doi:10.5194/acp-6-3181-2006, 2006.
- 16 Guo, H., Xu, L., Bougiatioti, A., Cerully, K.M., Capps, S.L., Hite Jr., J.R., Carlton, A.G., Lee, S.-.,  
17 Bergin, M.H., Ng, N.L., Nenes, A. and Weber, R.J.: Fine-particle water and pH in the  
18 southeastern United States, 15, 5211-5228, doi:10.5194/acp-15-5211-2015, 2015.
- 19 Hallquist, M., Wenger, J.C., Baltensperger, U., Rudich, Y., Simpson, D., Claeys, M., Dommen, J.,  
20 Donahue, N.M., George, C., Goldstein, A.H., Hamilton, J.F., Herrmann, H., Hoffmann, T.,  
21 Iinuma, Y., Jang, M., Jenkin, M.E., Jimenez, J.L., Kiendler-Scharr, A., Maenhaut, W.,  
22 McFiggans, G., Mentel, T.F., Monod, A., Prevot, A.S.H., Seinfeld, J.H., Surratt, J.D.,  
23 Szmigielski, R. and Wildt, J.: The formation, properties and impact of secondary organic aerosol:  
24 current and emerging issues, *Atmos. Chem. Phys.*, 9, 5155-5236, doi:10.5194/acp-9-5155-2009,  
25 2009.
- 26 Hayes, P. L., Ortega, A.M., Cubison, M.J., Froyd, K.D., Zhao, Y., Cliff, S.S., Hu, W.W., Toohey,  
27 D.W., Flynn, J.H., Lefer, B.L., Grossberg, N., Alvarez, S., Rappenglück, B., Taylor, J.W., Allan,  
28 J.D., Holloway, J.S., Gilman, J.B., Kuster, W.C., de Gouw, J.A., Massoli, P., Zhang, X., Liu, J.,  
29 Weber, R.J., Corrigan, A.L., Russell, L.M., Isaacman, G., Worton, D.R., Kreisberg, N.M.,  
30 Goldstein, A.H., Thalman, R., Waxman, E.M., Volkamer, R., Lin, Y.H., Surratt, J.D.,  
31 Kleindienst, T.E., Offenberg, J.H., Dusanter, S., Griffith, S., Stevens, P.S., Brioude, J., Angevine,  
32 W.M. and Jimenez, J.L.: Organic aerosol composition and sources in Pasadena, California during  
33 the 2010 CalNex campaign, *J. Geophys. Res.*, 118, 9233-9233, doi:10.1002/jgrd.50530, 2013.
- 34 Hsu, S. O. -, Ito, K. and Lippmann, M.: Effects of thoracic and fine PM and their components on heart  
35 rate and pulmonary function in COPD patients, *J Expos Sci Environ Epidemiol*, 21, 464-472,  
36 2011.
- 37 IPCC 2013, *Climate Change 2013: The Physical Science Basis, Contribution of Working Group I to*  
38 *the Fifth Assessment Report to the Intergovernmental Panel on Climate Change*, Cambridge  
39 University Press, Cambridge, United Kingdom and New York, NY, USA.
- 40 Jacobs, M. I., Darer, A.I. and Elrod, M.J.: Rate Constants and Products of the OH Reaction with  
41 Isoprene-Derived Epoxides, *Environ.Sci.Technol.*, 47, 12868-12876, doi:10.1021/es403340g,  
42 2013.

- 1 Jang, M., Czoschke, N.M., Lee, S. and Kamens, R.M.: Heterogeneous Atmospheric Aerosol  
2 Production by Acid-Catalyzed Particle-Phase Reactions, *Science*, 298, 814-817,  
3 doi:10.1126/science.1075798, 2002.
- 4 Jimenez, J. L., Canagaratna, M.R., Donahue, N.M., Prevot, A.S.H., Zhang, Q., Kroll, J.H., DeCarlo,  
5 P.F., Allan, J.D., Coe, H., Ng, N.L., Aiken, A.C., Docherty, K.S., Ulbrich, I.M., Grieshop, A.P.,  
6 Robinson, A.L., Duplissy, J., Smith, J.D., Wilson, K.R., Lanz, V.A., Hueglin, C., Sun, Y.L.,  
7 Tian, J., Laaksonen, A., Raatikainen, T., Rautiainen, J., Vaattovaara, P., Ehn, M., Kulmala, M.,  
8 Tomlinson, J.M., Collins, D.R., Cubison, M.J., E., Dunlea, J., Huffman, J.A., Onasch, T.B.,  
9 Alfarra, M.R., Williams, P.I., Bower, K., Kondo, Y., Schneider, J., Drewnick, F., Borrmann, S.,  
10 Weimer, S., Demerjian, K., Salcedo, D., Cottrell, L., Griffin, R., Takami, A., Miyoshi, T.,  
11 Hatakeyama, S., Shimono, A., Sun, J.Y., Zhang, Y.M., Dzepina, K., Kimmel, J.R., Sueper, D.,  
12 Jayne, J.T., Herndon, S.C., Trimborn, A.M., Williams, L.R., Wood, E.C., Middlebrook, A.M.,  
13 Kolb, C.E., Baltensperger, U. and Worsnop, D.R.: Evolution of Organic Aerosols in the  
14 Atmosphere. *Science*, 326, 1525-1529, doi:10.1126/science.1180353, 2009.
- 15 Jordan, A., Haidacher, S., Hanel, G., Hartungen, E., Herbig, J., Märk, L., Schottkowsky, R.,  
16 Seehauser, H., Sulzer, P. and Märk, T.D.: An online ultra-high sensitivity Proton-transfer-  
17 reaction mass-spectrometer combined with switchable reagent ion capability (PTR + SRI – MS),  
18 *Int. J. Mass. Spectrom.*, 286, 32-38, doi:<http://dx.doi.org/10.1016/j.ijms.2009.06.006>, 2009a.
- 19 Jordan, A., Haidacher, S., Hanel, G., Hartungen, E., Märk, L., Seehauser, H., Schottkowsky, R.,  
20 Sulzer, P. and Märk, T.D.: A high resolution and high sensitivity proton-transfer-reaction time-  
21 of-flight mass spectrometer (PTR-TOF-MS), *Int. J. Mass. Spectrom.*, 286, 122-128,  
22 doi:<http://dx.doi.org/10.1016/j.ijms.2009.07.005>, 2009b.
- 23 Kalberer, M., Paulsen, D., Sax, M., Steinbacher, M., Dommen, J., Prevot, A.S.H., Fisseha, R.,  
24 Weingartner, E., Frankevich, V., Zenobi, R. and Baltensperger, U.: Identification of Polymers as  
25 Major Components of Atmospheric Organic Aerosols, *Science*, 303, 1659-1662, 2004.
- 26 Kamens, R. M., Gery, M.W., Jeffries, H.E., Jackson, M. and Cole, E.I.: Ozone/isoprene reactions:  
27 Product formation and aerosol potential, *Int J Chem Kinet*, 14, 955-975,  
28 doi:10.1002/kin.550140902, 1982.
- 29 Karambelas, A., Pye, H.O.T., Budisulistiorini, S.H., Surratt, J.D. and Pinder, R.W.: Contribution of  
30 Isoprene Epoxydiol to Urban Organic Aerosol: Evidence from Modeling and Measurements,  
31 *Environ. Sci. Technol. Lett.*, 1, 278-283, doi:10.1021/ez5001353, 2014.
- 32 Ke, L., Ding, X., Tanner, R.L., Schauer, J.J. and Zheng, M.: Source contributions to carbonaceous  
33 aerosols in the Tennessee Valley Region, *Atmos. Environ.*, 41, 8898-8923,  
34 doi:10.1016/j.atmosenv.2007.08.024, 2007.
- 35 Kourtchev, I., Copolovici, L., Claeys, M. and Maenhaut, W.: Characterization of Atmospheric  
36 Aerosols at a Forested Site in Central Europe, *Environ.Sci.Technol.*, 43, 4665-4671,  
37 doi:10.1021/es803055w, 2009.
- 38 Kroll, J. H., Ng, N.L., Murphy, S.M., Flagan, R.C. and Seinfeld, J.H.: Secondary Organic Aerosol  
39 Formation from Isoprene Photooxidation, *Environ.Sci.Technol.*, 40, 1869-1877, 2006.
- 40 Lewis, C. W., Klouda, G.A. and Ellenson, W.D.: Radiocarbon measurement of the biogenic  
41 contribution to summertime PM-2.5 ambient aerosol in Nashville, TN, *Atmos. Environ.*, 38,  
42 6053-6061, doi:10.1016/j.atmosenv.2004.06.011, 2004.

- 1 Lin, Y. -, Knipping, E.M., Edgerton, E.S., Shaw, S.L. and Surratt, J.D.: Investigating the influences of  
2 SO<sub>2</sub> and NH<sub>3</sub> levels on isoprene-derived secondary organic aerosol formation using conditional  
3 sampling approaches, *Atmos. Chem. Phys.*, 13, 3095-3134, doi:10.5194/acp-13-8457-2013,  
4 2013a.
- 5 Lin, Y., Budisulistiorini, S.H., Chu, K., Siejack, R.A., Zhang, H., Riva, M., Zhang, Z., Gold, A.,  
6 Kautzman, K.E. and Surratt, J.D.: Light-Absorbing Oligomer Formation in Secondary Organic  
7 Aerosol from Reactive Uptake of Isoprene Epoxydiols, *Environ.Sci.Technol.*, 48, 12012-12021,  
8 doi:10.1021/es503142b, 2014.
- 9 Lin, Y., Zhang, H., Pye, H.O.T., Zhang, Z., Marth, W.J., Park, S., Arashiro, M., Cui, T.,  
10 Budisulistiorini, S.H., Sexton, K.G., Vizuete, W., Xie, Y., Luecken, D.J., Piletic, I.R., Edney,  
11 E.O., Bartolotti, L.J., Gold, A. and Surratt, J.D.: Epoxide as a precursor to secondary organic  
12 aerosol formation from isoprene photooxidation in the presence of nitrogen oxides, *Proc. Natl.*  
13 *Acad. Sci.*, doi:10.1073/pnas.1221150110, 2013b.
- 14 Lin, Y., Zhang, Z., Docherty, K.S., Zhang, H., Budisulistiorini, S.H., Rubitschun, C.L., Shaw, S.L.,  
15 Knipping, E.M., Edgerton, E.S., Kleindienst, T.E., Gold, A. and Surratt, J.D.: Isoprene  
16 Epoxydiols as Precursors to Secondary Organic Aerosol Formation: Acid-Catalyzed Reactive  
17 Uptake Studies with Authentic Compounds, *Environ. Sci. Technol.*, 46, 250-258,  
18 doi:10.1021/es202554c, 2012.
- 19 Liu, Y. J., Herdinger-Blatt, I., McKinney, K.A. and Martin, S.T.: Production of methyl vinyl ketone  
20 and methacrolein via the hydroperoxyl pathway of isoprene oxidation, *Atmos. Chem. Phys.*, 13,  
21 5715-5730, doi:10.5194/acp-13-5715-2013, 2013.
- 22 Liu, Y., Kuwata, M., Strick, B.F., Thomson, R.J., Geiger, F.M., McKinney, K. and Martin, S.T.:  
23 Uptake of Epoxydiol Isomers Accounts for Half of the Particle-Phase Material Produced from  
24 Isoprene Photooxidation via the HO<sub>2</sub> pathway, *Environ.Sci.Technol.*, doi:10.1021/es5034298,  
25 2014.
- 26 Mauderly, J. L. and Chow, J.C.: Health Effects of Organic Aerosols, *Inhal.Toxicol.*, 20, 257-288,  
27 doi:10.1080/08958370701866008, 2008.
- 28 McNeill, V. F., Woo, J.L., Kim, D.D., Schwier, A.N., Wannell, N.J., Sumner, A.J. and Barakat, J.M.:  
29 Aqueous-Phase Secondary Organic Aerosol and Organosulfate Formation in Atmospheric  
30 Aerosols: A Modeling Study, *Environ.Sci.Technol.*, 46, 8075-8081, doi:10.1021/es3002986,  
31 2012.
- 32 Middlebrook, A. M., Bahreini, R., Jimenez, J.L. and Canagaratna, M.R.: Evaluation of Composition-  
33 Dependent Collection Efficiencies for the Aerodyne Aerosol Mass Spectrometer using Field  
34 Data, *Aerosol Sci. Technol.*, 46, 258-271, doi:10.1080/02786826.2011.620041, 2012.
- 35 Nenes, A., Pandis, S.N. and Pilinis, C.: Continued development and testing of a new thermodynamic  
36 aerosol module for urban and regional air quality models, *Atmos.Environ.*, 33, 1553-1560,  
37 doi:10.1016/S1352-2310(98)00352-5, 1999.
- 38 Ng, N. L., Canagaratna, M.R., Jimenez, J.L., Zhang, Q., Ulbrich, I.M. and Worsnop, D.R.: Real-Time  
39 Methods for Estimating Organic Component Mass Concentrations from Aerosol Mass  
40 Spectrometer Data, *Environ. Sci. Technol.*, 45, 910-916, doi:10.1021/es102951k, 2011.

- 1 Nguyen, T. B., Coggon, M.M., Bates, K.H., Zhang, X., Schwantes, R.H., Schilling, K.A., Loza, C.L.,  
2 Flagan, R.C., Wennberg, P.O. and Seinfeld, J.H.: Organic aerosol formation from the reactive  
3 uptake of isoprene epoxydiols (IEPOX) onto non-acidified inorganic seeds, *Atmos. Chem. Phys.*,  
4 14, 3497-3510, doi:10.5194/acp-14-3497-2014, 2014.
- 5 Nguyen, T. B., Roach, P.J., Laskin, J., Laskin, A. and Nizkorodov, S.A.: Effect of humidity on the  
6 composition of isoprene photooxidation secondary organic aerosol, *Atmos. Chem. Phys.*, 11,  
7 6931-6944, doi:10.5194/acp-11-6931-2011, 2011.
- 8 Nguyen, T. B., Bates, K.H., Crouse, J.D., Schwantes, R.H., Zhang, X., Kjaergaard, H., Surratt, J.D.,  
9 Lin, P., Laskin, A., Seinfeld, J.H. and Wennberg, P.O.: Mechanism of the hydroxyl radical  
10 oxidation of methacryloyl peroxyxynitrate (MPAN) and its pathway toward secondary organic  
11 aerosol formation in the atmosphere, *Phys.Chem.Chem.Phys.*, -, doi:10.1039/C5CP02001H",  
12 2015.
- 13 Odum, J. R., Hoffmann, T., Bowman, F., Collins, D., Flagan, R.C. and Seinfeld, J.H.: Gas/Particle  
14 Partitioning and Secondary Organic Aerosol Yields, *Environ. Sci. Technol.*, 30, 2580-2585,  
15 doi:10.1021/es950943+, 1996.
- 16 Paatero, P. and Tapper, U.: Positive matrix factorization: A non-negative factor model with optimal  
17 utilization of error estimates of data values, *Environmetrics*, 5, 111-126,  
18 doi:10.1002/env.3170050203, 1994.
- 19 Pandis, S. N., Paulson, S.E., Seinfeld, J.H. and Flagan, R.C.: Aerosol formation in the photooxidation  
20 of isoprene and  $\beta$ -pinene, *Atmos. Environ.*, 25, 997-1008,  
21 doi:[http://dx.doi.org.libproxy.lib.unc.edu/10.1016/0960-1686\(91\)90141-S](http://dx.doi.org.libproxy.lib.unc.edu/10.1016/0960-1686(91)90141-S), 1991.
- 22 Pankow, J. F.: An absorption model of gas/particle partitioning of organic compounds in the  
23 atmosphere, *Atmos.Environ.*, 28, 185-188, doi:10.1016/1352-2310(94)90093-0, 1994.
- 24 Paulot, F., Crouse, J.D., Kjaergaard, H.G., Kürten, A., St. Clair, J.M., Seinfeld, J.H. and Wennberg,  
25 P.O.: Unexpected Epoxide Formation in the Gas-Phase Photooxidation of Isoprene, *Science*, 325,  
26 730-733, doi:10.1126/science.1172910, 2009.
- 27 Pye, H. O. T., Pinder, R.W., Piletic, I.R., Xie, Y., Capps, S.L., Lin, Y., Surratt, J.D., Zhang, Z., Gold,  
28 A., Luecken, D.J., Hutzell, W.T., Jaoui, M., Offenberg, J.H., Kleindienst, T.E., Lewandowski, M.  
29 and Edney, E.O.: Epoxide Pathways Improve Model Predictions of Isoprene Markers and Reveal  
30 Key Role of Acidity in Aerosol Formation, *Environ.Sci.Technol.*, 47, 11056-11064,  
31 doi:10.1021/es402106h, 2013.
- 32 Riedel, T. P., Lin, Y., Budisulistiorini, S.H., Gaston, C.J., Thornton, J.A., Zhang, Z., Vizuete, W.,  
33 Gold, A. and Surratt, J.D.: Heterogeneous reactions of isoprene-derived epoxides: reaction  
34 probabilities and molar secondary organic aerosol yield estimates, *Environ. Sci. Technol. Lett.*,  
35 doi:10.1021/ez500406f, 2015.
- 36 Robinson, N. H., Hamilton, J.F., Allan, J.D., Langford, B., Oram, D.E., Chen, Q., Docherty, K.,  
37 Farmer, D.K., Jimenez, J.L., Ward, M.W., Hewitt, C.N., Barley, M.H., Jenkin, M.E., Rickard,  
38 A.R., Martin, S.T., McFiggans, G. and Coe, H.: Evidence for a significant proportion of  
39 Secondary Organic Aerosol from isoprene above a maritime tropical forest, *Atmos. Chem. Phys.*,  
40 11, 1039-1050, doi:10.5194/acp-11-1039-2011, 2011.

- 1 Schichtel, B. A., Malm, W.C., Bench, G., Fallon, S., McDade, C.E., Chow, J.C. and Watson, J.G.:  
2 Fossil and contemporary fine particulate carbon fractions at 12 rural and urban sites in the United  
3 States, *J. Geophys. Res.*, 113, D02311, doi:10.1029/2007JD008605, 2008.
- 4 Schindelka, J., Iinuma, Y., Hoffmann, D. and Herrmann, H.: Sulfate radical-initiated formation of  
5 isoprene-derived organosulfates in atmospheric aerosols, *Faraday Discuss.*, 165, 237-259,  
6 doi:10.1039/C3FD00042G", 2013.
- 7 Schwartz, S.: Mass-Transport Considerations Pertinent to Aqueous Phase Reactions of Gases in  
8 Liquid-Water Clouds, 6, 415-471, doi:10.1007/978-3-642-70627-1\_16, 1986.
- 9 Slowik, J. G., Brook, J., Chang, R.Y.-., Evans, G.J., Hayden, K., Jeong, C.-., Li, S.-., Liggio, J., Liu,  
10 P.S.K., McGuire, M., Mihele, C., Sjostedt, S., Vlasenko, A. and Abbatt, J.P.D.: Photochemical  
11 processing of organic aerosol at nearby continental sites: contrast between urban plumes and  
12 regional aerosol, *Atmos. Chem. Phys.*, 11, 2991-3006, doi:10.5194/acp-11-2991-2011, 2011.
- 13 Sun, Y., Zhang, Q., Zheng, M., Ding, X., Edgerton, E.S. and Wang, X.: Characterization and Source  
14 Apportionment of Water-Soluble Organic Matter in Atmospheric Fine Particles (PM<sub>2.5</sub>) with  
15 High-Resolution Aerosol Mass Spectrometry and GC-MS, *Environ.Sci.Technol.*, 45, 4854-4861,  
16 doi:10.1021/es200162h, 2011.
- 17 Surratt, J. D., Chan, A.W.H., Eddingsaas, N.C., Chan, M., Loza, C.L., Kwan, A.J., Hersey, S.P.,  
18 Flagan, R.C., Wennberg, P.O. and Seinfeld, J.H.: Reactive intermediates revealed in secondary  
19 organic aerosol formation from isoprene, *Proc. Natl. Acad. Sci.*, 107, 6640-6645,  
20 doi:10.1073/pnas.0911114107, 2010.
- 21 Surratt, J. D., Gomez-Gonzalez, Y., Chan, A.W.H., Vermeylen, R., Shahgholi, M., Kleindienst,  
22 T.E., Edney, E.O., Offenberg, J.H., Lewandowski, M., Jaoui, M., Maenhaut, W., Claeys, M.,  
23 Flagan, R.C. and Seinfeld, J.H.: Organosulfate Formation in Biogenic Secondary Organic  
24 Aerosol, *J Phys Chem A*, 112, 8345-8378, doi:10.1021/jp802310p, 2008.
- 25 Surratt, J. D., Kroll, J.H., Kleindienst, T.E., Edney, E.O., Claeys, M., Sorooshian, A., Ng, N.L.,  
26 Offenberg, J.H., Lewandowski, M., Jaoui, M., Flagan, R.C. and Seinfeld, J.H.: Evidence for  
27 Organosulfates in Secondary Organic Aerosol, *Environ. Sci. Technol.*, 41, 517-527,  
28 doi:10.1021/es062081q, 2007a.
- 29 Surratt, J. D., Lewandowski, M., Offenberg, J.H., Jaoui, M., Kleindienst, T.E., Edney, E.O. and  
30 Seinfeld, J.H.: Effect of Acidity on Secondary Organic Aerosol Formation from Isoprene,  
31 *Environ.Sci.Technol.*, 41, 5363-5369, doi:10.1021/es0704176, 2007b.
- 32 Surratt, J. D., Murphy, S.M., Kroll, J.H., Ng, N.L., Hildebrandt, L., Sorooshian, A., Szmigielski, R.,  
33 Vermeylen, R., Maenhaut, W., Claeys, M., Flagan, R.C. and Seinfeld, J.H.: Chemical  
34 Composition of Secondary Organic Aerosol Formed from the Photooxidation of Isoprene, *J Phys  
35 Chem A*, 110, 9665-9690, doi:10.1021/jp061734m, 2006.
- 36 Tanner, R. L., Bairai, S.T. and Mueller, S.F.: Trends in concentrations of atmospheric gaseous and  
37 particulate species in rural eastern Tennessee as related to primary emissions reductions, *Atmos.  
38 Chem. Phys. Discuss.*, 15, 13211-13262, doi:10.5194/acpd-15-13211-2015, 2015.
- 39 Tanner, R. L., Bairai, S.T., Olszyna, K.J., Valente, M.L. and Valente, R.J.: Diurnal patterns in PM<sub>2.5</sub>  
40 mass and composition at a background, complex terrain site, *Atmos.Environ.*, 39, 3865-3875,  
41 doi:10.1016/j.atmosenv.2005.03.014, 2005.

- 1 Tanner, R. L., Parkhurst, W.J. and McNichol, A.P.: Fossil Sources of Ambient Aerosol Carbon Based  
2 on <sup>14</sup>C Measurements Special Issue of Aerosol Science and Technology on Findings from the  
3 Fine Particulate Matter Supersites Program, *Aerosol Sci. Technol.*, 38, 133-139,  
4 doi:10.1080/02786820390229453, 2004.
- 5 Tolocka, M. P., Jang, M., Ginter, J.M., Cox, F.J., Kamens, R.M. and Johnston, M.V.: Formation of  
6 Oligomers in Secondary Organic Aerosol, *Environ.Sci.Technol.*, 38, 1428-1434,  
7 doi:10.1021/es035030r, 2004.
- 8 Turpin, B. J. and Lim, H.J.: Species Contributions to PM<sub>2.5</sub> Mass Concentrations: Revisiting  
9 Common Assumptions for Estimating Organic Mass, *Aerosol Sci. Technol.*, 35, 602-610,  
10 doi:10.1080/02786820119445, 2001.
- 11 Ulbrich, I. M., Canagaratna, M.R., Zhang, Q., Worsnop, D.R. and Jimenez, J.L.: Interpretation of  
12 organic components from Positive Matrix Factorization of aerosol mass spectrometric data,  
13 *Atmos. Chem. Phys.*, 9, 2891-2918, 2009.
- 14 Veres, P., Roberts, J.M., Warneke, C., Welsh-Bon, D., Zahniser, M., Herndon, S., Fall, R. and de  
15 Gouw, J.: Development of negative-ion proton-transfer chemical-ionization mass spectrometry  
16 (NI-PT-CIMS) for the measurement of gas-phase organic acids in the atmosphere, *Int. J. Mass*  
17 *spectrom.*, 274, 48-55, doi:<http://dx.doi.org/10.1016/j.ijms.2008.04.032>, 2008.
- 18 Wang, W., Kourtchev, I., Graham, B., Cafmeyer, J., Maenhaut, W. and Claeys, M.: Characterization  
19 of oxygenated derivatives of isoprene related to 2-methyltetrols in Amazonian aerosols using  
20 trimethylsilylation and gas chromatography/ion trap mass spectrometry, *Rapid Commun.Mass*  
21 *Spectrom.*, 19, 1343-1351, doi:10.1002/rcm.1940, 2005.
- 22 Woo, J. L. and McNeill, V.F.: simpleGAMMA 1.0 – A reduced model of secondary organic aerosol  
23 formation in the aqueous aerosol phase (aaSOA), *Geosci. Model Dev.*, 8, 1821-1829,  
24 doi:10.5194/gmdd-8-463-2015, 2015.
- 25 Worton, D. R., Surratt, J.D., LaFranchi, B.W., Chan, A.W.H., Zhao, Y., Weber, R.J., Park, J., Gilman,  
26 J.B., de Gouw, J., Park, C., Schade, G., Beaver, M., Clair, J.M.S., Crounse, J., Wennberg, P.,  
27 Wolfe, G.M., Harrold, S., Thornton, J.A., Farmer, D.K., Docherty, K.S., Cubison, M.J., Jimenez,  
28 J., Frossard, A.A., Russell, L.M., Kristensen, K., Glasius, M., Mao, J., Ren, X., Brune, W.,  
29 Browne, E.C., Pusede, S.E., Cohen, R.C., Seinfeld, J.H. and Goldstein, A.H.: Observational  
30 Insights into Aerosol Formation from Isoprene, *Environ.Sci.Technol.*, 47, 11403-11413,  
31 doi:10.1021/es4011064, 2013.
- 32 Xu, L., Guo, H., Boyd, C.M., Klein, M., Bougiatioti, A., Cerully, K.M., Hite, J.R., Isaacman-  
33 VanWertz, G., Kreisberg, N.M., Knote, C., Olson, K., Koss, A., Goldstein, A.H., Hering, S.V., de  
34 Gouw, J., Baumann, K., Lee, S., Nenes, A., Weber, R.J. and Ng, N.L.: Effects of anthropogenic  
35 emissions on aerosol formation from isoprene and monoterpenes in the southeastern United  
36 States, *Proc. Natl. Acad. Sci.*, 112, 37-42, doi:10.1073/pnas.1417609112, 2015.
- 37 You, Y., Renbaum-Wolff, L., Carreras-Sospedra, M., Hanna, S.J., Hiranuma, N., Kamal, S., Smith,  
38 M.L., Zhang, X., Weber, R.J., Shilling, J.E., Dabdub, D., Martin, S.T. and Bertram, A.K.: Images  
39 reveal that atmospheric particles can undergo liquid-liquid phase separations, *Proc. Natl. Acad.*  
40 *Sci.*, 109, 13188-13193, doi:10.1073/pnas.1206414109, 2012.
- 41 Zhang, H., Surratt, J.D., Lin, Y.H., Bapat, J. and Kamens, R.M.: Effect of relative humidity on SOA  
42 formation from isoprene/NO photooxidation: enhancement of 2-methylglyceric acid and its

1 corresponding oligoesters under dry conditions, *Atmos. Chem. Phys.*, 11, 6411-6424,  
2 doi:10.5194/acp-11-6411-2011, 2011.

3 Zhang, X., Liu, Z., Hecobian, A., Zheng, M., Frank, N.H., Edgerton, E.S. and Weber, R.J.: Spatial and  
4 seasonal variations of fine particle water-soluble organic carbon (WSOC) over the southeastern  
5 United States: implications for secondary organic aerosol formation, *Atmos. Chem. Phys.*, 12,  
6 6593-6607, doi:10.5194/acp-12-6593-2012, 2012a.

7 Zhang, Z., Lin, Y.H., Zhang, H., Surratt, J.D., Ball, L.M. and Gold, A.: Technical Note: Synthesis of  
8 isoprene atmospheric oxidation products: isomeric epoxydiols and the rearrangement products  
9 cis- and trans-3-methyl-3,4-dihydroxytetrahydrofuran, *Atmos. Chem. Phys.*, 12, 8529-8535,  
10 doi:10.5194/acp-12-8529-2012, 2012b.

11

12

1 **Table 1.** Summary of isoprene-derived SOA tracers measured by GC/EI-MS and  
 2 UPLC/DAD-ESI-HR-QTOFMS

SOA Tracers	Retention Time (min)	# of Samples Detected <sup>a</sup>	Concentration (ng m <sup>-3</sup> )		Average % among detected tracers
			Maximum	Mean	
<b>Tracers by GC/EI-MS</b>					
<i>trans</i> -3-MeTHF-3,4-diol	20.5	55	18.8	2.7	0.2%
<i>cis</i> -3-MeTHF-3,4-diol	21.1	29	5.7	1.7	0.1%
2-methylglyceric acid	23.4	119	36.7	7.5	1.5%
2-methylthreitol	32.9	122	329.8	42.4	8.6%
2-methylerythritol	33.7	122	1269.7	120.7	24.4%
(Z)-2-methylbut-3-ene-1,2,4-triol	25.6	121	260.0	29.1	5.8%
2-methylbut-3-ene-1,2,3-triol	26.6	118	162.5	16.5	3.2%
(E)-2-methylbut-3-ene-1,2,4-triol	26.9	122	1127.0	98.8	19.9%
<b>Tracers by UPLC/DAD-ESI-HR-QTOFMS tracers</b>					
IEPOX-derived organosulfates	1.1–1.7	122	1135.3	169.5	34.2%
IEPOX-derived dimer organosulfate	2.8	103	14.0	1.4	0.2%
MAE-derived organosulfate	1.1	114	77.9	10.0	1.9%

3 <sup>a</sup> Total number of samples is 123

4 **Table 2.** Correlation ( $r^2$ ) of PMF Factors with isoprene-derived SOA tracers measured by  
 5 GC/EI-MS and UPLC/DAD-ESI-HR-QTOFMS

SOA Tracers	IEPOX-OA	LV-OOA	91Fac
3-methyltetrahydrofuran-3,4-diols	0.12	0.13	0.24
2-methyltetrols	0.80	0.20	0.38
C <sub>5</sub> -alkene triols	0.75	0.19	0.44
2-methylglyceric acid	0.38	0.44	0.44
IEPOX-derived organosulfates	0.76	0.29	0.42
IEPOX-derived dimer organosulfate	0.71	0.12	0.34
MAE-derived organosulfate	0.37	0.44	0.52

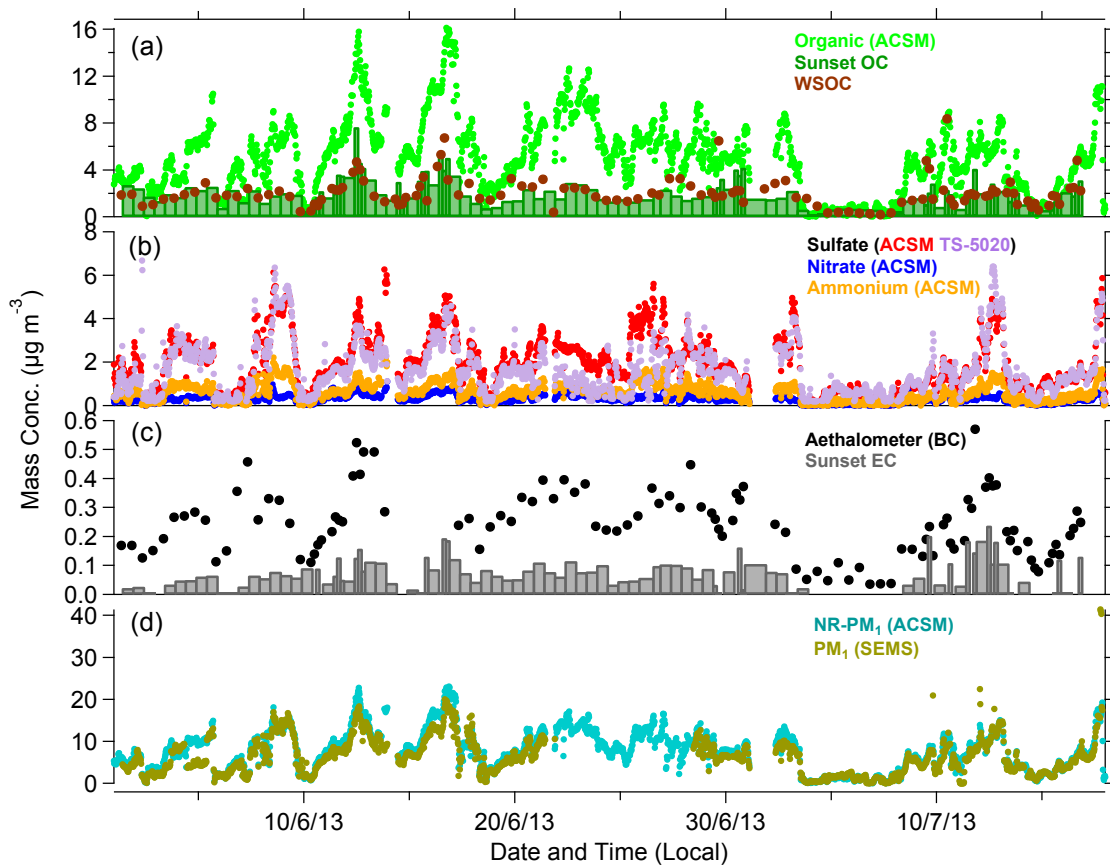
6

7 **Table 3.** Correlation ( $r^2$ ) of modeled SOA tracers with measurements

H* (M atm <sup>-1</sup> )	2-methyltetrols		IEPOX organosulfates	
	$r^2$	Slope	$r^2$	Slope
$3.0 \times 10^7$ <sup>a</sup>	0.45	9.61±0.91	0.66	10.65±0.73
$2.7 \times 10^6$ <sup>b</sup>	0.44	0.69±0.06	0.66	0.90±0.06

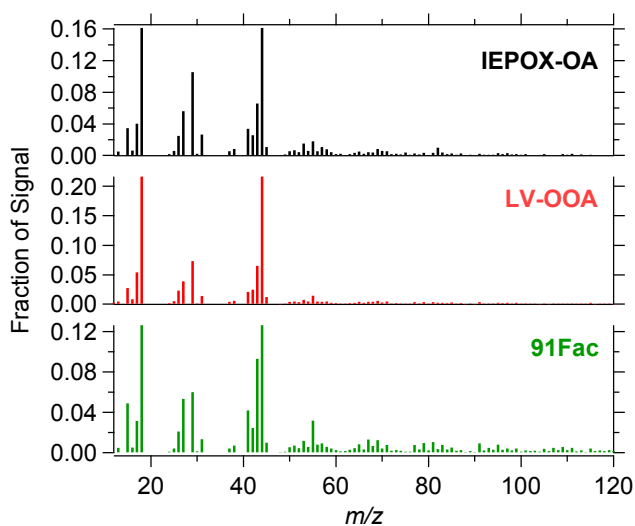
8 References: (a) Nguyen et al. (2014) and (b) Pye et al. (2013)

9

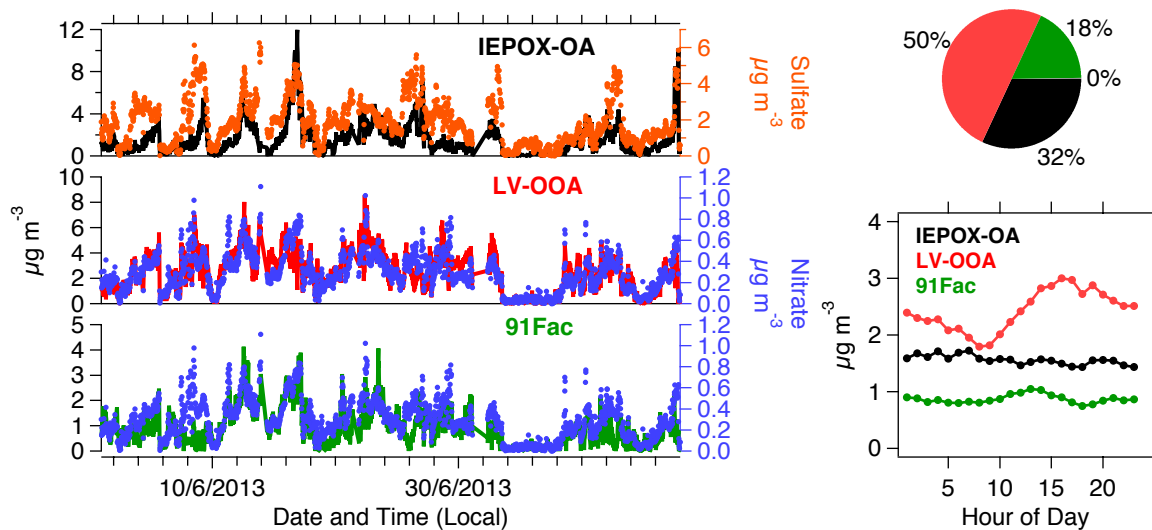


1  
 2 **Figure 1.** Time series mass concentration of (a) organic and (b) inorganics (excluding  
 3 chloride) measured by ACSM, (c) black carbon (BC) measured by Aethalometer, and (d) NR-  
 4 PM<sub>1</sub> and PM<sub>1</sub> mass concentrations measured by ACSM and SEMs-MCPC. Collocated sulfate  
 5 aerosol measured by Thermo Scientific Sulfate Analyzer was plotted on (b). OC (bars) and  
 6 WSOC (dots), both in unit of  $\mu\text{gC m}^{-3}$ , measured from filter samples were plotted on (a) with  
 7 ACSM organic. EC (bars; in unit of  $\mu\text{gC m}^{-3}$ ) measured from filter samples were plotted on  
 8 (c) along with BC measurements.

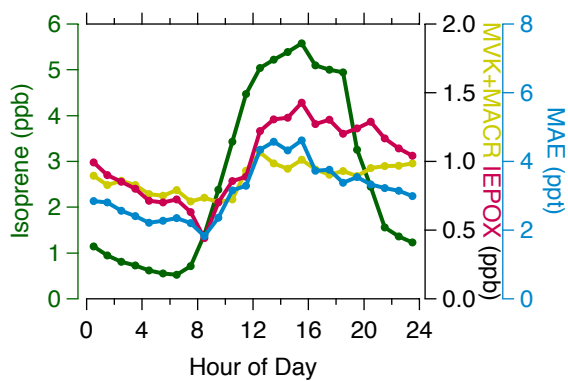
9  
 10



1  
 2 **Figure 2.** Mass spectra obtained for the 3-factor solution from PMF: IEPOX-OA, LV-OOA,  
 3 and 91 Fac.



4  
 5 **Figure 3.** Left panel shows the PMF 3-factor solution time series mass contributions  
 6 measured by ACSM. Top to bottom: left ordinate, IEPOX-OA (black), LV-OOA (red), and 91  
 7 Fac (green); right ordinate, sulfate (orange) and nitrate (blue). Right panel shows average  
 8 mass contributions (top) and diurnal variation (bottom) of factors resolved by PMF.

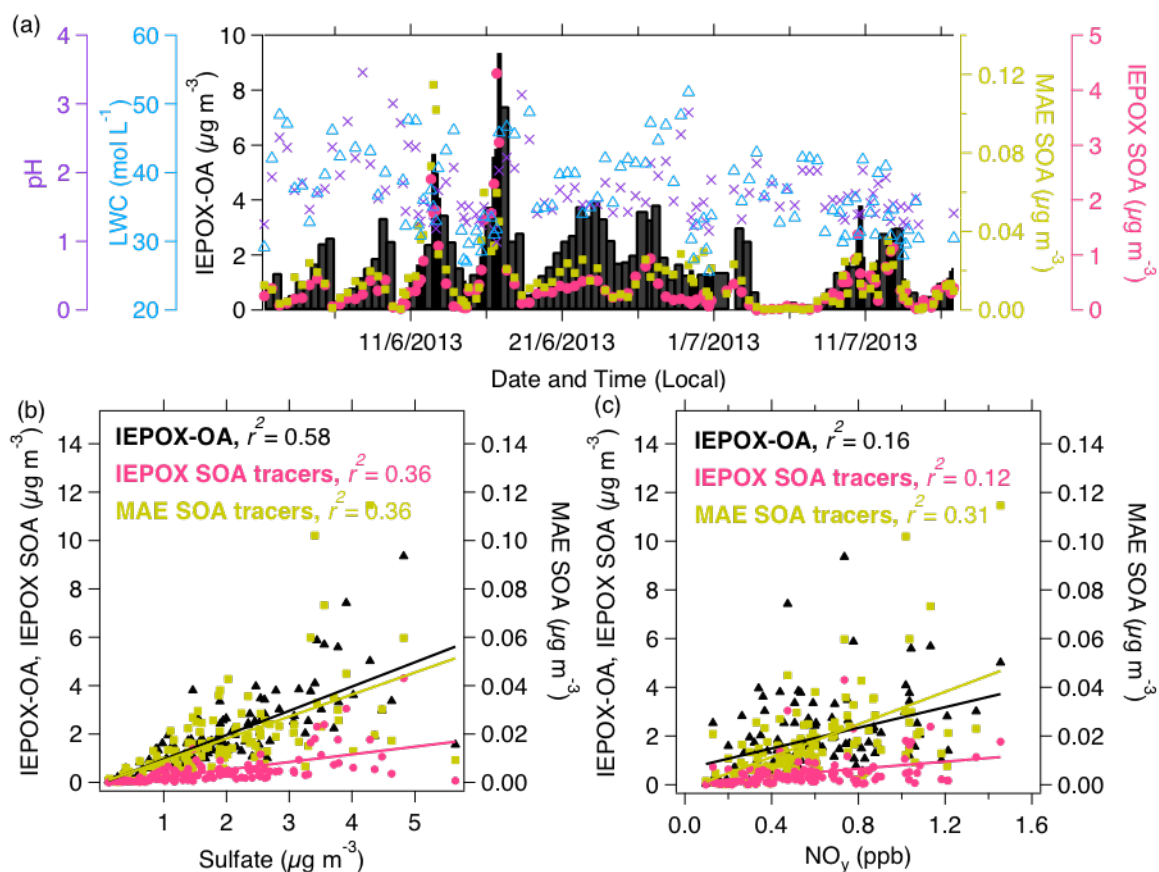


1  
 2 **Figure 4.** Diurnal variation of isoprene (left ordinate) as well as isoprene gaseous 3  
 3 photooxidation products (right ordinates), i.e., MVK+MACR, IEPOX and MAE, measured at  
 4 LRK site. It should be noted that IEPOX signal includes interference of ISOPOOH at  
 5 unknown ratio, thus its mixing ratio represents an upper limit.

6

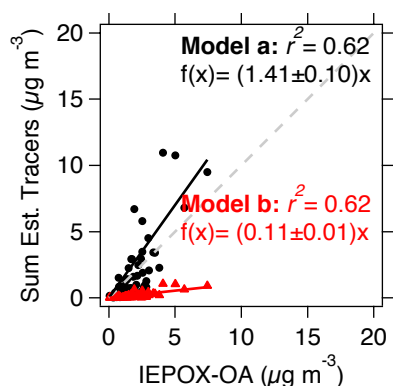
7

8



1  
 2 **Figure 5.** (a) Time series of IEPOX-OA factor (black bars; darker bars are intensive filter  
 3 sampling periods), sum of IEPOX-derived (pink circle) and MAE-derived (yellow square)  
 4 SOA tracers, aerosol pH (purple cross) and LWC (blue triangle) estimated by ISORROPIA-II  
 5 model. Campaign average pH and LWC are  $1.78 \pm 0.53$  and  $38.71 \pm 7.43$  mol L<sup>-1</sup>, respectively.  
 6 Correlation plots between IEPOX-OA, summed of IEPOX- and MAE-derived SOA tracers  
 7 and (b) sulfate measurements by ACSM and (c) NO<sub>y</sub> measurements from NPS.

8



1  
 2 **Figure 6.** Correlation of summed IEPOX-derived SOA tracers estimated by simpleGAMMA  
 3 by assuming  $H^*$  of  $3.0 \times 10^7$  (Nguyen et al., 2014) (model a) and  $2.7 \times 10^6$  (Pye et al.,  
 4 2013) (model b) and IEPOX-OA factor from PMF analysis.

5

6